Accepted Manuscript

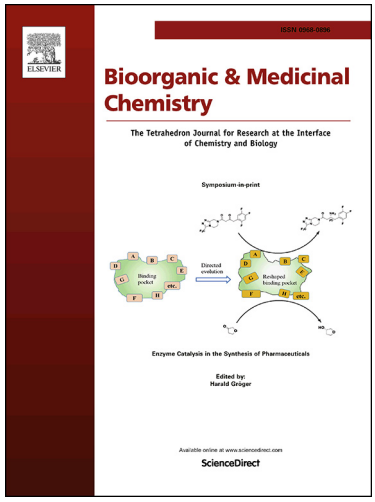

Novel multi-target directed ligands based on annelated xanthine scaffold with aromatic substituents acting on adenosine receptor and monoamine oxidase B. Synthesis, *in vitro* and *in sillico* studies

Michał Załuski, Jakub Schabikowski, Miriam Schlenk, Agnieszka Olejarz-Maciej, Bartłomiej Kubas, Tadeusz Karcz, Kamil Kuder, Gniewomir Latacz, Małgorzata Zygmunt, David Synak, Sonja Hinz, Christa E. Müller, Katarzyna Kieć-Kononowicz

PII: S0968-0896(18)32025-X
DOI: https://doi.org/10.1016/j.bmc.2019.02.004
Reference: BMC 14740

To appear in: *Bioorganic & Medicinal Chemistry*

Received Date: 4 December 2018
Revised Date: 25 January 2019
Accepted Date: 1 February 2019

Please cite this article as: Załuski, M., Schabikowski, J., Schlenk, M., Olejarz-Maciej, A., Kubas, B., Karcz, T., Kuder, K., Latacz, G., Zygmunt, M., Synak, D., Hinz, S., Müller, C.E., Kieć-Kononowicz, K., Novel multi-target directed ligands based on annelated xanthine scaffold with aromatic substituents acting on adenosine receptor and monoamine oxidase B. Synthesis, *in vitro* and *in sillico* studies, *Bioorganic & Medicinal Chemistry* (2019), doi: https://doi.org/10.1016/j.bmc.2019.02.004

Novel multi-target directed ligands based on annelated xanthine scaffold with aromatic substituents acting on adenosine receptor and monoamine oxidase B. Synthesis, *in vitro* and *in sillico* studies.

[1]*Michał Załuski,* [1]*Jakub Schabikowski,* [3]*Miriam Schlenk,* [1]*Agnieszka Olejarz-Maciej,* [1]*Bartłomiej Kubas,* [1]*Tadeusz Karcz,* [1]*Kamil Kuder,* [1]*Gniewomir Latacz,* [2]*Małgorzata Zygmunt,* [1]*David Synak,* [3]*Sonja Hinz* [3]*Christa E. Müller,* [1]*Katarzyna Kieć-Kononowicz*

[1] Department of Technology and Biotechnology of Drugs, Faculty of Pharmacy, Jagiellonian University Medical College, Kraków, Poland

[2] Department of Pharmacodynamics, Faculty of Pharmacy, Jagiellonian University Medical College, Kraków, Poland.

[3]PharmaCenter Bonn, Pharmaceutical Institute, Pharmaceutical Chemistry I, University of Bonn, An der Immenburg 4, 53121 Bonn, Germany

*Correspondence: Katarzyna Kieć –Kononowicz, Department of Technology and Biotechnology of Drugs, Jagiellonian University Medical College, 9 Medyczna Street, 30-688 Kraków, Poland

E-mail address: *mfkonono@cyf-kr.edu.pl*

Tel/fax: +48-12- 6205580/ +48-12- 6205596

Keywords: adenosine A_{2A} receptors ligands, annelated xanthines, hepatotoxicity, molecular docking, monoamine oxidase B inhibitors, neurodegenerative diseases, Parkinson's disease,

Abstract

*N*9-benzyl-substituted imidazo-, pyrimido- and 1,3-diazepino[2,1-*f*]purinediones were designed as dual-target-directed ligands combining A_{2A} adenosine receptor (AR) antagonistic activity with blockade of monoamine oxidase B (MAO-B). A library of 37 novel compounds was synthesized and biologically evaluated in radioligand binding studies at AR subtypes and for their ability to inhibit MAO-B. A systematic modification of the tricyclic structures based on a xanthine core by enlargement of the third heterocyclic ring or attachment of various substituted benzyl moieties resulted in the development of 9-(2-chloro-6-fluorobenzyl)-1,3-dimethyl-6,7,8,9-tetrahydropyrimido[2,1-*f*]purine-2,4(1*H*,3*H*)-dione (**9u**; K_i human A_{2A}AR: 189 nM and IC_{50} human MAO-B: 570 nM) as the most potent dual acting ligand of the series displaying high selectivity versus related targets. Moreover, some potent, selective MAO-B inhibitors were identified in the group of pyrimido- and 1,3- diazepino[2,1-*f*]purinediones. Compound **10d** (10-(3,4-dichlorobenzyl)-1,3-dimethyl-7,8,9,10-tetrahydro-1*H*-[1,3]diazepino[2,1-*f*]purine-2,4(3*H*,6*H*)-dione) displayed an IC_{50} value at human MAO-B of 83 nM. Analysis of structure-activity relationships was complemented by molecular docking studies based on previously published X-ray structures of the protein targets. An extended biological profile was determined for selected compounds including *in vitro* evaluation of potential hepatotoxicity calculated *in silico* and antioxidant properties as an additional desirable activity. The new molecules acting as dual target drugs may provide symptomatic relief as well as disease-modifying effects for neurodegenerative diseases, in particular Parkinson's disease.

1. Introduction

Neurodegenerative diseases (NDs) such as Alzheimer's, Parkinson's, and Huntington's disease and amyotrophic lateral sclerosis (AD, PD, HD, ALS respectively) are complex and multi-factorial disorders with unclear onset and continuous progression, caused by genetic, environmental and endogenous pathogenic factors.[1–4] The characteristic symptom of NDs is selective neuronal degeneration having various molecular mechanisms and presenting different clinical manifestations. However, some general pathways leading to neuronal death such as protein misfolding and aggregation, oxidative stress and free radical formation, metal dyshomeostasis, mitochondrial dysfunction and phosphorylation impairment occur concurrently in those disorders.[5–8]

Despite continuous progression in the understanding of the biochemical aspects of NDs, the current therapeutic efficacy is still limited to palliative and/or symptomatic effects. Moreover, molecules interacting with a single known biological target appear to be insufficient to fully prevent, retard, halt or reverse NDs.[2,8,9] Therefore, alternative approaches such as the development of multi target-directed ligands (MTDLs) have recently gained considerable attention. The concept of MTDLs suggests one molecule interacting with two or more precisely defined biological targets with the aim to increase therapeutic efficacy. This approach presents a wide range of advantages related to pharmacokinetic and pharmacodynamic profiles, reducing drug-drug interactions and improving patient compliance as compared to polypharmacology by combination of drugs or single-pill drug combinations.[8,10]

In the context of MTDLs designed for the treatment of NDs, molecules possessing both neuroprotective and symptomatic effects seem to be especially desirable. Adenosine A_{2A} receptors and monoamine oxidase B are used as targets for the treatment of neurodegenerative disorders, however recent studies indicate, as they provide not only symptomatic relief but may also mediate neuroprotective effect.[11]

Monoamine oxidase B (MAO-B) is an isoform of the enzyme catalyzing the oxidative deamination of endogenous and xenobiotic amines and thereby reducing levels of biogenic amine neurotransmitters in the CNS.[12] Some studies suggest that elevated levels of MAO-B in the aging brain accelerate the neurodegenerative process since potentially neurotoxic substances such as dopaldehyde and hydrogen peroxide are formed as by-product of the reaction catalyzed by this enzyme. These reactive compounds may lead to neuronal death by oxidation of nucleic acids or proteins causing oxidative damage due to Fenton's reaction by forming hydroxyl radicals.[8,13–15] Considering the abovementioned reasons, MAO-B inhibitors, which are already well established therapeutics for PD, seem to be interesting candidates for the development of MTDLs potentially exhibiting disease-modifying activity in NDs. Actually, selective MAO-B inhibitors such as: selegiline (**1a**), rasagiline (**1b**) or safinamide (**1c**) are already applied as adjunctive therapeutics for PD in order to elevate dopamine concentration in the brain [16–18]. (Fig 1.)

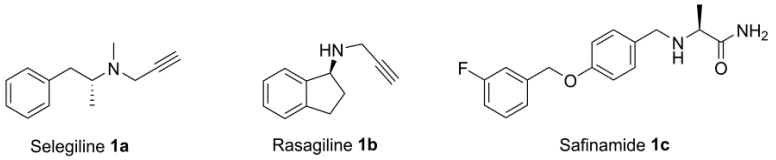

Figure 1 Structures of potent MAO-B inhibitors

Adenosine A_{2A} receptors (A_{2A}ARs) are one of the four subtypes of adenosine receptors which are subdivided into A_1, A_{2A}, A_{2B}, and A_3ARs belonging to the G protein-coupled receptor (GPCR) family. A_{2A}ARs are highly expressed in specific areas of the brain, such as

the caudate-putamen.[19,20] Blockade of A_{2A}ARs has resulted in neuroprotective effects in preclinical studies by different cellular mechanism. A_{2A}AR antagonists have beneficial impact on the enhancement of D_2-dopaminergic transmission related to PD and also reduce side effects of L-DOPA therapy.[21–24] Moreover, there is evidence that blockade of the A_{2A}AR reduces β-amyloid peptide aggregation [23,25].

Based on those considerations, structures with dual target activity as A_{2A} AR antagonists and MAO-B inhibitors may have potential application in PD or AD possibly providing both symptomatic and neuroprotective effects. Therefore, the development of new A_{2A}AR/MAO-B dual targeted structures has been promoted, in particular among structures based on a xanthine scaffold, however non-xanthine compounds have been also reported.[26–28]

Caffeine (**2a**) and theophyline (**2b**) are naturally occurring unselective AR antagonists from the group of methylxanthines. The structural modification of the xanthine scaffold, especially in position 8, led to the discovery of the group of 8-styrylxanthines, among which istradefylline (**3a**) and 8-chlorostyrylcaffeine (CSC, **3b**) were obtained [24]. Istradefylline is a potent and selective A_{2A}AR antagonist, that has been approved in Japan for the treatment of Parkinson's disease as an adjunct therapy [29], while CSC is one of the first known antagonists of A_{2A}AR with ancillary MAO-B inhibitory activity [28]. (Fig 2.)

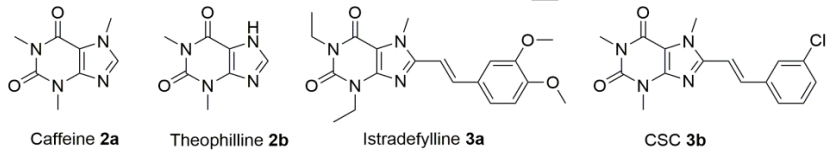

Figure 2 Structures of xanthine derivatives as adenosine receptors antagonists.

The class of tricyclic compounds containing a third ring fused to the *f*-bond of the 2,6-purinedione system with a benzyl residue can be considered as bioisosteric analogues of (*E*)-8-styrylxanthine. Therefore, the annelated xanthine derivatives with pyrimido[2,1-*f*]purinediones scaffold were investigated as AR ligands by our group as well as by others.[30–32] Koch et al. have reported structure **4** in this class of compounds as A_1/A_{2A}ARs antagonist with ancillary MAO-B inhibitory activity. They suggested the crucial role of substituents in *N*1,*N*3-position of xanthine core for triple-target activity. 1,3-dimethylpyrimido[2,1-*f*]purinedione derivatives **5** seem to be suitable for both A_{2A} AR antagonism and MAO-B inhibition, while structures with longer substituents in the *N*3 position such as propargyl presented higher affinity for ARs while the potency at MAO-B was decreased[33]. (Fig. 3)

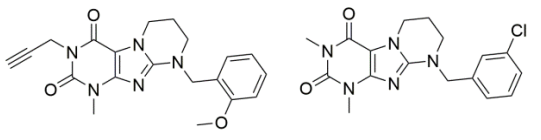

Figure 3 Pyrimido[2,1-*f*]purinediones derivatives as multiple target directed ligands.

Considering the abovementioned evidences, we made efforts to develop new dual target structures as A_{2A} antagonists/MAO-B inhibitors with enhanced and more balanced potencies. As a suitable scaffold, annelated 1,3-dimethylxanthines with the imidazole, pyrimidine or diazepine ring fused to the *f*-bond were selected. The investigation of structure-activity relationships in the group of tricyclic compounds with an aromatic residue attached

by a short one/two carbon spacer was performed. Furthermore, we evaluated the impact of the size of the heterocyclic ring fused to xanthine core on inhibition of MAO-B and affinity for A_{2A}ARs. To rationalize the observed biological activities of the new compounds, molecular docking studies using human A_{2A} ARs and human MAO-B were performed. Moreover, MAO-A inhibition potency was determined for some tricyclic xanthine derivatives, and their MAO-B selectivity was evaluated. For all final products, selected molecular and ADMET (absorption, distribution, metabolism, excretion, toxicity) properties were estimated by *in silico* calculation. and the most active structures were tested *in vitro* for hepatotoxic and antioxidant effects.

2. Results and discussion

2.1. Chemistry

The synthesis of tricyclic 1,3-dimethyl-imidazo-, pyrimido-, and diazepino[2,1-*f*]purinediones with an aromatic residue in the 8-, 9-, or 10-position, respectively, of the annelated xanthine was performed by a three-step procedure as shown in Scheme 1. The diversity by different aromatic residues was introduced in the last step of the synthetic pathway during the ring closure reaction with various aromatic amines.

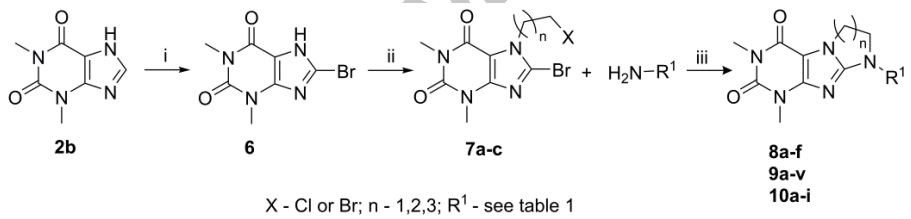

Scheme 1 Synthesis of tricyclic xanthine derivatives) 40 % HBr, $NaClO_3$, CH_3COOH, 60 °C; ii) 1,2-dibromoethane/1-bromo-3-chloropropane/1,4-dibromobutane, Benzyltriethylammonium chloride TEBA, K_2CO_3, acetone, reflux, 10h; iii) 1-propanol, NEt_3, µM, 300W, 160 °C.

As a starting material, theophylline (**2b**) was oxidatively brominated according to a previously described method [34]. Subsequently, 8-bromotheophylline (**6**) was subjected to *N*7-alkylation with dihalogenoalkane such as 1,2-dibromoethane, 1-bromo-3-chloropropane or 1,4-dibromobutane. Phase transfer catalysis reaction conditions were applied providing 8-bromo-7-(2-bromoethyl)theophylline (**7a**), 8-bromo-7-(3-chloropropyl)theophylline (**7b**) or 8-bromo-7-(4-bromobutyl)theophylline (**7c**).[35] The last step of the synthetic pathway was the condensation **7a-c** with an appropriate amine providing the final tricyclic xanthine derivatives in the series of 1,3-dimethyl-imidazo- (**8a-f**), pyrimido- **(9a-v)**, and diazepino-[2,1-*f*]purinediones (**10a-i**). Previously we had described a conventional approach for the ring-closure reactions, which required long refluxing time in high boiling solvents such as diethyleneglycol monomethyl ether or DMF [30]. Now we decided to use microwave irradiation and sealed vessels to reduce the time of the reaction. This approach allowed us to provide during 1 hour good reaction yields compared to 16h required upon conventional heating.

The structures of all new synthesized compounds were confirmed by spectral analysis including ^{1}H NMR, ^{13}C NMR, and MS. The melting points were determined for all new compounds. The purity of all tested compounds was determined to be at least 95 % using UPLC coupled to MS.

2.2. Biological evaluation

The final compounds were tested in radioligand binding assays to evaluate their affinity for all ARs subtypes. Rat brain cortical membranes were used for determining rat A_1 AR affinity. Human A_{2A} and A_{2B} were recombinantly expressed in HEK293 cells. Human A_1 and human A_3ARs were recombinantly expressed in Chinese hamster ovary (CHO) cells. [^{3}H]2-Chloro-N^6-cyclopentyladenosine ([^{3}H]CCPA) [36], [^{3}H]3-(3-hydroxypropyl)-1-propargyl-7-methyl-8-(*m*-methoxystyryl)xanthine ([^{3}H]MSX-2) [37], [^{3}H]8-(4-(4-(4-chlorophenyl)piperazine-1-sulfonyl)phenyl)-1-propylxanthine ([^{3}H]PSB-603) [38] and [^{3}H]2-phenyl-8-ethyl-4-methyl-(8*R*)-4,5,7,8-tetrahydro-1*H*-imidazo[2,1-*i*]purine-5-one ([^{3}H]PSB-11) [39] were used as radioligands for A_1, A_{2A}, A_{2B} and A_3 AR binding studies, respectively. Several previous studies on pyrimido[2,1-*f*]purinediones had shown that compounds belonging to this group displayed antagonistic properties for ARs.[30,33] All new compounds were tested for inhibitory potency at human MAO-B**.** Selected compounds were additionally tested for selectivity versus human MAO-A.

Table 1 Adenosine receptors affinity of tricyclic compounds and xanthine derivatives

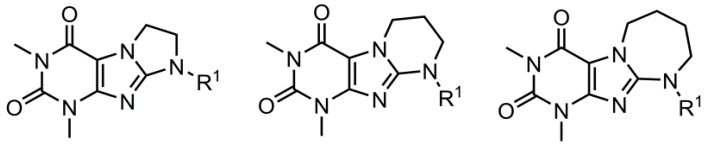

Compd	R^1	A_1 vs. [^{3}H]CCPA (h, human; r, rat)	A_{2A} vs. [^{3}H]MSX-2 (h, human; r, rat)	A_{2B} vs. ^{3}H]PSB-603	A_3 vs. [^{3}H]PSB-11
			K_i ± SEM (μM) (or % inhibition ± SEM at 1 μM)		
Caffeine **2a** [40]		44.9 [h] 41.0 [r]	23.4 [h] 32.5 [r]	33.8 [h]	13.3 [h]
Istradefylline **3a** [40]		0.841 [h] 0.230 [r]	0.0912 [h] 0.0044 [r]	>10.0 [h]	4.47 [h]
KD240 5 [33,41]		>10.0 [h] (21%) 0.432 ± 0.027 [r] 1.42 ± 0.08 [r]	2.03 ± 0.16 [h] 0.802 ± 0.156 [r] 1.12 ± 0.14 [r]	>1.00 (10%)	15.2 ± 5.5
	Imidazo[2,1-*f*]purinedione				
8a	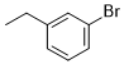	**0.396** ± 0.134	**0.369** ± 0.115	>1.0 (30 ± 4)	>1.0 (22 ± 10)
8b	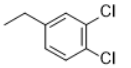	>1.0 (1 ± 1)	>1.0 (29 ± 8)	>1.0 (22 ± 11)	>1.0 (11 ± 7)
8c		>1.0 (24 ± 3)	**0.887** ± 0.214	>1.0 (21 ± 0)	>1.0 (37 ± 2)
8d	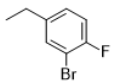	>1.0 (6 ± 11)	>1.0 (30 ± 7)	>1.0 (2 ± 1)	>1.0 (1 ± 5)
8e	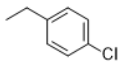	>1.0 (23 ± 2)	>1.0 (42 ± 4)	>1.0 (21 ± 0)	>1.0 (30 ± 9)

8f		>1.0 (30 ± 1)	**0.784** ± 0.107	>1.0 (3 ± 6)	>1.0 (15 ± 0)
	Pyrimido[2,1-*f*]purinedione				
9a		1.780 ± 0.420 [r]	1.210 ± 0.250	>1.0	>1.0
9b	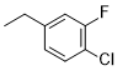	>1.0 [r]	>1.0	>1.0	>1.0
9c	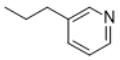	>1.0 [r]	3.040 ± 0.440	>1.0	>1.0
9d	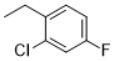	>1.0 [r]	>1.0	>1.0	>1.0
9e	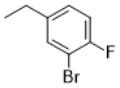	4.360 ± 0.400 [r]	8.270 ± 0.144	>1.0	>1.0
9f	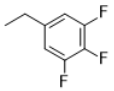	>1.0 [r]	>1.0	>1.0	>1.0
9g		2.650 ± 0.640 [r]	2.020 ± 0.290	>1.0	>1.0
9h	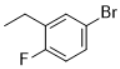	**0.486** ± 0.022 [r]	>1.0	>1.0	>1.0
9i	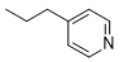	>1.0 [r]	>1.0	>1.0	>1.0
9j	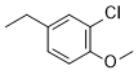	>1.0 [r]	8.000 ± 1.890	>1.0	>1.0
9k	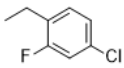	4.900 ± 0.280 [r]	8.910 ± 2.310	>1.0	>1.0
9l	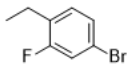	4.130 ± 1.340 [r]	>1.0	>1.0	>1.0
9m	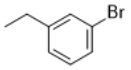	0.965 ± 0.087 [r]	1.700 ± 0.090	>1.0	>1.0
9n		2.320 ± 0.130 [r]	1.610 ± 0.255	>1.0	>1.0
9o	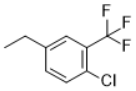	>1.0 [r]	>1.0	>1.0	>1.0
9p	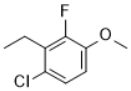	0.927 ± 0.207 [r]	**0.627** ± 0.078	>1.0	>1.0
9q	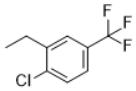	0.931 ± 0.242 [r]	>1.0	>1.0	>1.0
9r	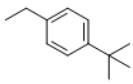	>1.0 [r]	>1.0	>1.0	>1.0

9s		1.410 ± 0.278 [r]	1.020 ± 0.275	>1.0	>1.0
9t	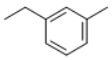	1.910 ± 0.648 [r]	>1.0	>1.0	>1.0
9u		1.550 ± 0.310 [r]	**0.189** ± 0.047	>1.0	>1.0
9v	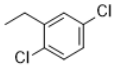	3.020 ± 0.067 [r]	>1.0	>1.0	>1.0
	Diazepino[2,1-*f*]purinedione				
10a		>1.0 (10 ± 7)	**0.881** ± 0.087	>1.0 (41 ± 9)	>1.0 (15 ± 3)
10b		>1.0 (11 ± 1)	1080 ± 350 (42 ± 14)	>1.0 (40 ± 1)	>1.0 (11 ± 1)
10c	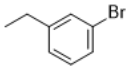	**0.651** ± 0.057	>1.0 (41 ± 6)	>1.0 (41 ± 2)	>1.0 (26 ± 2)
10d	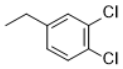	>1.0 (21 ± 2)	>1.0 (33 ± 1)	>1.0 (40 ± 2)	>1.0 (26 ± 4)
10e		>1.0 (21 ± 3)	**0.767** ± 0.115	>1.0 (43 ± 3)	>1.0 (42 ± 7)
10f	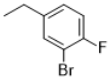	>1.0 (23 ± 4)	>1.0 (30 ± 5)	>1.0 (43 ± 3)	>1.0 (20 ± 7)
10g		>1.0 (13 ± 4)	**0.959** ± 0.154	>1.0 (16 ± 4)	>1.0 (19 ± 10)
10h	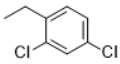	>1.0 (16 ± 4)	1.580 ± 0.413 (52 ± 7)	>1.0 (5 ± 3)	>1.0 (31 ± 9)
10i	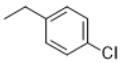	>1.0 (13 ± 7)	>1.0 (9 ± 5)	>1.0 (13 ± 3)	>1.0 (10 ± 4)

2.3. Structure-activity relationships at adenosine receptors

From a structural point of view, the synthesized compounds can be subdivided into three series according to the kind of the third heterocyclic ring fused to the xanthine core: 1) *N*8-substituted 1,3-dimethylimidazo[2,1-*f*]purinediones, 2) *N*9-substituted 1,3-dimethylpyrimido[2,1-*f*]purinediones, 3) *N*10-substituted 1,3-dimethyldiazepino[2,1-*f*]purinediones. Their affinities for ARs are presented in Table **1.**

Within the three series, all investigated derivatives showed no affinity for the human A_{2B} and A_3 ARs at the highest tested concentration. In general, most of the compounds presented none or only negligible affinity for the A_1 AR. Only the dual active structure **8a** possesses activity with a K_i value of approximately 0.4 µM for both human A_1 and A_{2A}AR. Modification of this compound by the enlargement of the third heterocyclic ring (**9m** and **10c**)

resulted in a decrease in affinity for both biological targets. Shifting of the bromine atom in the aromatic ring (**8c**, **9n**, **10c**, **10e**) led to a drop in affinity for A_{2A}ARs in all series, however in contrast to the imidazo[2,1-*f*]purinediones, *ortho*-Br-substituted diazepino[2,1-*f*]purinodione (**10e**) derivatives presented slightly higher affinity than *meta*-Br derivative (**10c**). Within other mono-substituted structures *para*-Cl (**8e**, **10i**), *ortho*-F (**9b**, **10b**), *ortho*-methyl (**9s**), *meta*-methyl (**9t**), and *para*-isopropyl (**9r**) were less well tolerated than bromine containing derivatives. Exceptions were the *ortho*-methoxy (**8f**, **10g**) and *ortho*-Cl (**10a**) substituted compounds, which presented comparable affinity for the A_{2A} AR with K_i values slightly below 1 µM similar to the *ortho*-Br analogues.

In order to evaluate the structural determinants for interaction with the A_{2A} AR in more detail, di/tri-substituted benzyl derivatives of the tricyclic xanthines were investigated. Within the group of di-substituted compounds, 2,4-dichloro (**10h**), 3,4-dichloro (**8b**, **10d**) and 2,5-dichloro (**9v**) displayed low affinity for the A_{2A} AR with *K*i values in the micromolar range . However, replacement of one atom - chlorine or fluorine in the 2,6-disubstitued compound (**9u**) increased the affinity remarkably (A_{2A}: 0.185 µM). Further modification of the substitution pattern of the aromatic ring containing two halogen atoms (**8d**, **9b**, **9d**, **9e**, **9h**, **9k**, **9l**, **10f**) resulted in a reduction of affinity to micromolar values. The same effect was also observed for 2/4-chloro-5-trifluoromethyl (**9o**, **9q**) and 3-chloro-4-methoxy substituents.

Introduction of a 2-fluoro-3-methoxy-6-chlorobenzyl residue in the *N*9-position, as a modification of the potent 2-chloro-6-fluoro derivative, decreased the affinity for A_{2A} AR by three-fold. Compared to compound **9u**, structure **9p** presented a K_i value three fold lower. Another *N*9-tri-substituted benzyl-1,3-dimethylpyrimido[2,1-*f*]purinedione, **9f**, displayed low affinity for the A_{2A} AR.

A further strategy was to replace the benzene ring by aromatic heterocyclic ones. However, introduction of the bioisosteric 2-thienylmethyl moiety (**9g**) or 3/4-ethylpyridine residues (**9c**, **9i**) did not improve affinity for the A_{2A} AR.

2.4. Structure-activity relationship at MAO

All compounds were evaluated for their human MAO-B inhibitory potencies. Moreover, selectivity toward human MAO-A was additionally investigated for selected structures. The results for MAO-A and MAO-B are presented in Table 2.

Within three series, none of the selected compounds was found to inhibit MAO-A by 50 % or higher at the highest tested concentration of 1 or 100 µM. Therefore, all of the compounds that were found to inhibit MAO-B are selective versus MAO-A.

In the series of 1,3-dimethylpyrimido[2,1-*f*]purinediones, structures with IC_{50}-values in nanomolar range were found in the group *N*9-benzyl-substituted derivatives. Replacement of the benzyl residue by a bioisosteric 2-thienylmethyl moiety (**9g**) or 3/4-ethylpyridine resulted in a drop in inhibitory activity. Within *N*9-benzyl-substituted 1,3-dimethylpyrimido[2,1-*f*]purinediones derivatives, the most potent compound was **9n** bearing an *ortho*-Br-benzyl moiety (IC_{50} human MAO-B = 150 nM). Other *ortho*-mono-substituted derivatives (**9f**, **9s**) were also relatively potent in the following rank order of potency: Br > Cl > F > methyl. Generally, a shift of the substituent to the *meta*-position (**9m**) was slightly less tolerated, however *meta*-methyl derivatives (**9t**) displayed higher inhibitory activity of MAO-

B than an *ortho*-methyl analogue (**9s**). The analysis of structure-activity relationships in the other two series was consistent with the results described above (**8a**, **8c**, **8f**, **10a-c**, **10e**, **10g**). Additionally, the *para*-mono-substituted compounds (**8e**, **10i**) presented similar activity as the *meta*-substituted analogues. Furthermore, the series of *N*8-substituted benzyl-1,3-dimethylimidazo[2,1-*f*]purinediones seems to be less preferable for MAO-B inhibition compared to the *N*9-substituted benzyl-1,3-dimethylpyrimido[2,1-*f*]purinediones and the *N*10-substituted benzyl-1,3-dimethyldiazepino[2,1-*f*]purinediones, those displayed comparable results.

Among the group of di-substituted compounds, 2,4- and3,4-disubstituted derivatives with two halogen atoms or one halogen atom and a trifluoromethyl or methoxy group proved to be suitable for MAO-B inhibition. The most potent compound was **10d** bearing a 3,4-dichloro-benzyl moiety and a seven-membered heterocyclic ring fused to the xanthine core. Replacement of chlorine atoms by fluorine or bromine (**10f**) in 3,4-di-substituted structures resulted in a slight decrease of activity. The same observation was true for compound **10h** with one chlorine atom in the benzene ring shifted from the 3- to the 2-position. Further modification of 2,4- and 3,4-di-substituted benzyl derivatives (**9b**, **9d-e**, **9j-l**, **10f**) did not improve inhibitory activity, on the other hand they still maintained IC_{50}-values for the enzyme in the nanomolar range for both series: 1,3-dimethylpyrimido[2,1-*f*]purinedione and 1,3-dimethyldiazepino[2,1-*f*]purinedione derivatives. Nevertheless, in the series of 1,3-dimethylimidazo[2,1-*f*]purinediones, compound **8d** with a 3-bromo-4-fluorobenzyl moiety showed higher activity that the 3,4-dichlorobenzyl derivative (**8b**). A drop of activity was also observed for 2,4-di- and tri-substituted benzyl compounds within all series.

Compound **9u**, which was characterized as the most potent A_{2A} AR ligand among all investigated series, displayed also MAO-B inhibitory activity (IC_{50} human MAO-B = 570 nM). However, the 2-chloro-6-fluoro-substituted structure **9u** and its derivative with a 2-fluoro-3-methoxy-6-chlorobenzyl moiety (**9p**) were less active at MAO-B than 3,4-di-substituted benzyl derivatives.

Table 2 MAO A and B inhibitory activity of tricyclic xanthine derivatives; nd - not determined

Compd	IC_{50} ± SEM (μM) (or % inhibition ± SEM at 1 μM or 100 μM)	
	MAO-A	MAO-B
Rasagiline **1a**	nd	15.4
CSC **3b** [33]	>10.0	0.0178
5 [33,41]	nd	0.344
Imidazo[2,1-*f*]purinedione		
8a	> 1.0 (11 ± 1)	> 1.0 (39 ± 0)
8b	> 1.0 (-2 ± 1)	0.515 ± 0.030
8c	> 1.0 (13 ± 1)	0.991 ± 0.090
8d	> 1.0 (6 ± 1)	0.177 ± 0.012
8e	> 1.0 (16 ± 0)	>1.0 (42 ± 0)
8f	> 1.0 (7 ± 0)	111.0 ± 2.9
Pyrimido[2,1-*f*]purinedione		
9a	> 1.0 (-1 ± 3)	0.583 ± 0.209
9b	> 100.0 (9 ± 3)	0.264 ± 0.036
9c	nd	>1.0 (1 ± 1))

9d	nd	0.411 ± 0.050
9e	> 1.0 (1 ± 1)	0.346 ± 0.022
9f	nd	> 1.0 (24 ± 0)
9g	nd	>1.0 (20 ± 1)
9h	nd	1.18 ± 0.16
9i	nd	>1.0 (4 ± 1)
9j	> 100.0 (38 ± 1)	0.407 ± 0.085
9k	> 1.0 (2 ± 1.3)	0.377 ± 0.071
9l	> 1.0 (-2 ± 0.3)	0.426 ± 0.067
9m	> 1.0 (-1 ± 0.7)	0.396 ± 0.011
9n	> 1.0 (1 ± 1.2)	0.150 ± 0.039
9o	> 1.0 (2 ± 0.5)	0.310 ± 0.134
9p	> 100 (16 ± 5)	0.840 ± 0.025
9q	nd	1.070 ± 0.010
9r	nd	1.350 ± 0.050
9s	nd	>1.0 (40 ± 0)
9t	> 100 (17 ± 2)	0.313 ± 0.021
9u	> 100 (10 ± 0)	0.570 ± 0.018
9v	nd	0.758 ± 0.009
Diazepino[2,1-*f*]purinedione		
10a	> 1.0 (4 ± 1)	0.343 ± 0.028
10b	> 1.0 (14 ± 0)	>1.0 (39 ±1)
10c	> 1.0 (6 ± 0)	0.371 ± 0.031
10d	> 1.0 (5 ± 1)	0.083 ± 0.016
10e	> 1.0 (3 ± 0)	0.275 ± 0.050
10f	> 1.0 (-6 ± 1)	0.171 ± 0.009
10g	> 1.0 (2 ± 1)	1.917 ± 0.491
10h	> 1.0 (-2 ± 1)	0.282 ± 0.053
10i	> 1.0 (6 ± 1)	0.364 ± 0.006

2.5. Structure-activity relationships for both A_{2A} AR and MAO-B

The detailed analysis of SAR for each biological target was described above. Moreover, the global conclusion of structure-activity relationships within investigated library of compounds based on tricyclic core is assembled in Scheme 2 for both A_{2A} AR and MAO-B.

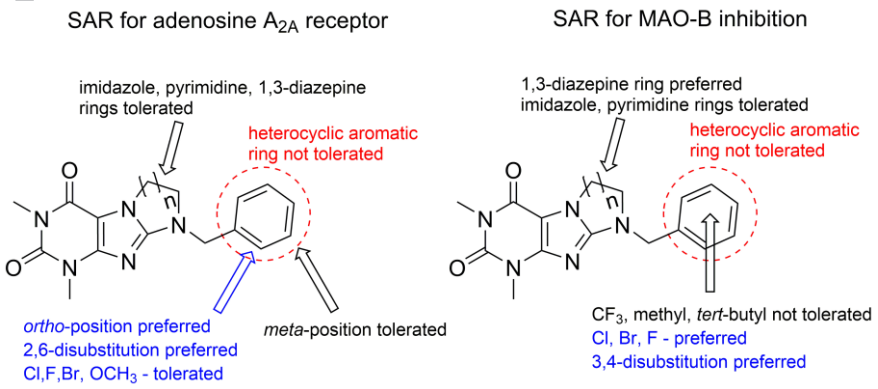

Scheme 2 Structure-activity relationships of tricyclic structures

2.6. Molecular modelling studies

2.6.1. Adenosine A_{2A} crystal structure

Among 34 X-ray structures of adenosine A_{2A} receptor complexes deposited in the PDB database, four are co-crystallized with xanthines: caffeine (PDB codes: 5MZP[42], 3RFM[43]), theophylline (PDB code: 5MZJ[42]) or XAC (PDB code: 3REY. The 3REY crystal structure was used for docking studies due to the similar size and structure of the described ligands.

In order to validate the methods used, XAC was redocked to its crystal structure. The superposition of the phenylpurinedione core with the co-crystallized ligand was almost ideal, although its flexible polar chain was bent towards the extracellular loop 2 (ECL2). As this occurrence was in agreement with previous findings [44], the implemented docking protocol was chosen for further docking studies. Detailed information on docking protocols can be found in “Experimental protocols” section.

All of the docked ligands can be grouped in two clusters. The highest ranked cluster 1 includes ligand poses where the purinedione core is rotated, yet with still overlapping carbonyl groups when compared to the XAC conformation in the crystal structure, in a way that ASN253$^{6.55}$ forms a hydrogen bond with the carbonyl group in position 2 of the purinedione core. In this position, the annelated heterocyclic rings, independent of size, point toward transmembrane helix 2 (TM2). Lower, but still highly ranked cluster 2 includes poses

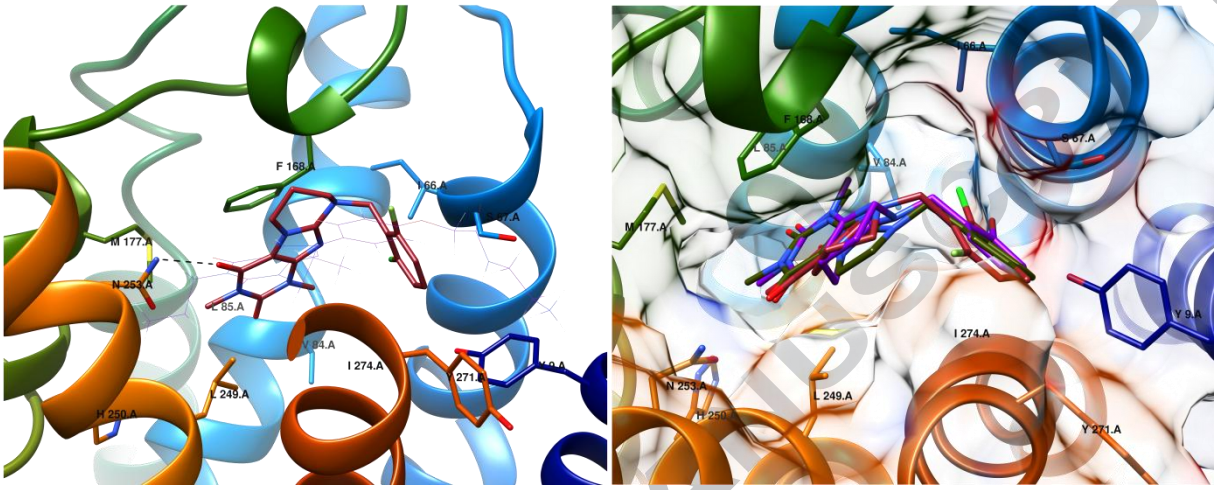

Figure 4 Left panel: calculated binding pose of 9u (dark red) in the 3REY binding pocket; native ligand XAC shown as violet wire. Right panel: top, surface view of superimposed calculated binding modes of 8a (green), 9u (dark red).

superimposing the whole phenylpurinedione core, as well as retaining the described ligand-receptor interactions of XAC: the terminal amino group of ASN 253$^{6.55}$ forms a hydrogen bond with the carbonyl group in position 6 of the purinedione core, that is stabilized through π- π stacking with the aromatic ring of PHE168 (ECL2). Paying attention to the poses and ligand-receptor interactions of xanthine derivatives in their co-crystallized complexes, it might be assumed that the binding mode of the ligands described herein in the adenosine A_{2A} receptor would reflect those of cluster 2 poses. Annelated heterocyclic rings, independent of size, are located in a narrow pocket formed by PHE 168 and GLU 169 (ECL2) from one side and TM7 amino acids MET 270$^{7.35}$ and ILE 274$^{7.39}$ from the other side, while substituted benzyl moieties are located between TYR9$^{1.35}$, SER67$^{2.65}$ and TYR271$^{7.36}$ (Fig. 4). No additional interactions between halogen and/or alkyl(oxy) substituents of the benzyl moiety were found for the most affine ligands from all of the subgroups. Therefore, no correlation between *in vitro* / and *in silico* results could be observed, and no explanation for the A_{2A} AR affinity of particular ligands could be found. However, it can be stated that all of the ligands fit well into the A_{2A} AR binding pocket forming the expected receptor-ligand interactions.

2.6.2. Monoamine oxidase B crystal structure

As there is no available crystal structure of MAO-B with co-crystallized xanthine derivatives, we used a structure with Safinamide in this studies (SAF; PDB ID: 2V5Z [45]), which shows some structural similarities (methylated aminoformamide fragment) to the purinedione core. An additional argument for using this as a model is documented by molecular docking studies carried out on 8-styrylcaffeine structures. According to literature

[28], the position of SAF within the binding pocket is as follows: the halogen-substituted aromatic ring lies within the entry cavity, while the polar fragment is housed in an aromatic cage and is directed towards the cofactor flavin adenine dinucleotide (FAD). Due to the structural analogy, a similar arrangement was expected for described herein ligands. Similar to previous target, and in order to validate the methods used, SAF was redocked to its crystal structure, and the resulting pose was perfectly superimposed with the native ligand, although the terminal amide moiety was flipped by 180^{o} horizontally.

All of the ligands fit well, and for most of the docked ligands, the substituted phenyl moiety is pointing towards the entry cavity, while the purinedione core fits between the cage, formed by TYR435 and GLN206 on one side, and TYR398 and LEU171 on the other side and is stabilized by π- π stacking with TYR326 and/or PHE343. Two binding modes of the purinedione core placement were found. One includes the N3-methyl group pointing toward TYR326/PHE343, as well as an additional halogen bond formation with THR201 for several compounds (e.g. **9n-9p**), while the phenyl ring is pointing towards the entrance cavity. The second binding mode differs by a deeper position of the ligands, in close proximity to the FAD. In this mode, the purinedione core is flipped horizontally and stabilized by π- π stacking with TYR 398, while the OH-group of TYR188 forms a hydrogen bond with the carbonyl group in position 6 of the core, along with additional π- π stacking interactions between the substituted phenyl ring and TYR326 (Fig. 5). This mode was observed for most of the highly affine pyrimido- and diazepino- annelated derivatives. It might be therefore assumed, that this binding mode will appear with higher probability, and the described interactions might influence the ligands' MAO-B affinity.

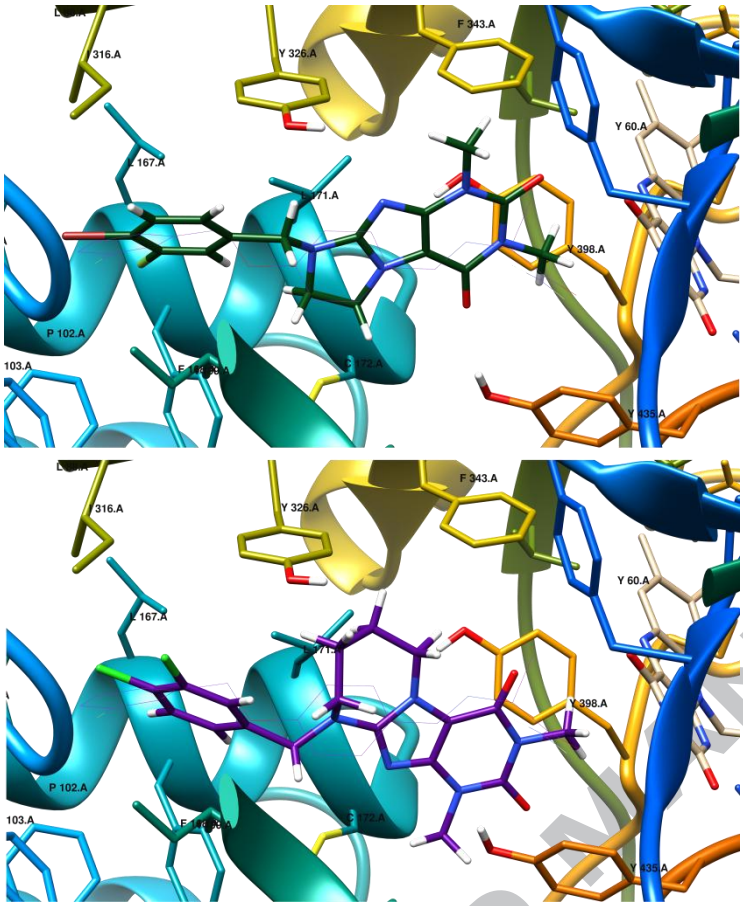

Figure 5 Calculated binding modes of **8d** (green; upper panel) and **10d** (violet; lower panel) superimposed with the ligand safinamide (SAF, violet, thin wire)

2.7. Blood brain barrier permeability

The final compounds were evaluated *in silico* for their ability to exceed blood brain barrier (BBB) as one of the most important parameter for structures acting in the CNS. The results are assembled in Table S2 (see Supplementary data). Most of investigated structures were estimated as potential able to penetrated across BBB. Only few compounds were found with BBB parameter indicating on poor permeability, probably associated with additional hydrogen bond acceptor group of these structures.

2.8. Hepatotoxicity of tricyclic structures

Prediction of selected drug-likeness parameters and ADME-Tox descriptors using Molinspiration and pkCSM software provided promising results, with the only problematic attribute that all compounds might be, according to the calculations, hepatotoxic. The details of the *in silico* calculations are given in the Supplementary data. Therefore, the most active compounds were also tested by *in vitro* studies to determine probable hepatotoxicity. Structures **9n**, **9u** and **10d** were incubated for 72 h with the *hepatoma* HepG2 cell line. For compounds **9n** and **9u** similar, statistically significant, antiproliferative effect ($p < 0.01$, < 0.001) were observed, but only at the highest dose used of 100 µM (Fig. 6).

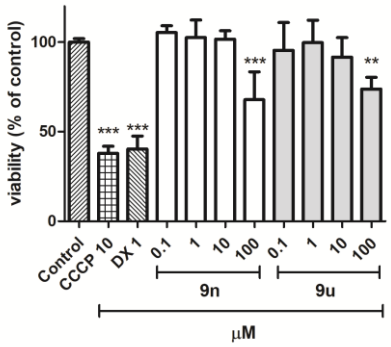

Figure 6 The effect of the cytostatic drug doxorubicin (DX), the mitochondrial toxin - carbonyl cyanide 3-chlorophenylhydrazone (CCCP), **9n** and **9u** on HepG2 cell viability. Statistical significance was evaluated by one-way ANOVA, followed by Bonferroni's comparison test (**p < 0.01, ***p < 0.001, compared with the negative control)**.**

Interestingly, *N*10-3,4-dicholorobenzyldiazepino[2,1-*f*]purinedione derivative **10d** was found as a very hepatotoxic agent. The statistically significant decrease of HepG2 cell viability was observed at low doses 0.5 μM ($p < 0.001$) and 1 μM ($p < 0.05$), respectively (Fig.7). Results from higher concentrations of 10 and 100 μM were not considered due to the observed compound precipitation in the cell culture media.

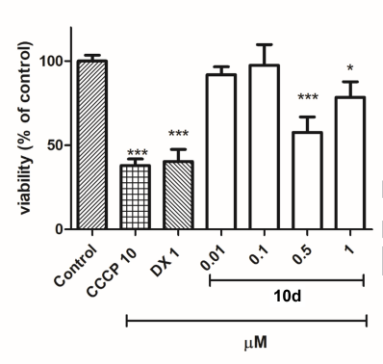

Figure 7 The effect of the cytostatic drug doxorubicin (DX), the mitochondrial toxin - carbonyl cyanide 3-chlorophenylhydrazone (CCCP) and **10d** on HepG2 cell viability. Statistical significance was evaluated by one-way ANOVA, followed by Bonferroni's comparison test (*p < 0.05, ***p < 0.001, compared with the negative control).

The hepatotoxicity determined in the *in vitro* assay was not fully correlated with *in silico* calculations. However, compound **10d** showed a strong hepatotoxic effect in contrast to structures **9n** and **9u**. Therefore, the tricyclic structures based on a xanthine scaffold may present a certain risk of hepatotoxicity as *in silico* study predicted. Nevertheless, the toxic effect seems to be dependent on structural modifications, especially in the attached substituted aromatic residue rather than the tricyclic core of the molecule.

2.9. Antioxidant activity of selected tricyclic compounds

Antioxidants and free radical scavengers may have beneficial effects for ND treatment as previously mentioned. Therefore, the selected compounds were tested in two assays to determine their potential antioxidant properties and the utility in protection from lipid peroxidation.

2.9.1. Determination of the antioxidant activity by the FRAP assay

Table 3. Influence of the test compounds on the total antioxidant activity *in vitro*

Compound	Absorption (%)
vitamin C	100
9n	3.40
10d	0.59

Compounds **9n**, **10d** were tested at a concentration 1000 μM. **9n** increased the total ferric-reducing antioxidant ability by 3.40%, while **10d** was practically inactive in this test (Table 3).

2.9.2. Influence of the test compounds on lipid peroxidation in rat brain homogenate

Table 4. Influence of the test compounds on lipid peroxidation

Compound	Absorption (%)
Carvedilol	44.8
9n	29.5
10d	16.6

Compounds **9n**, **10d** were tested at a concentration of 1000 μM. **9n** and **10d** inhibited lipid peroxidation by 29.5% and 16.6% respectively, (Table 4). This effect is not superior to the antioxidant activity of carvedilol, which has been used in this assays as reference compound. However, the results showed additional biological activity that combined with A_{2A} antagonism and MAO-B inhibition may provide synergistic neuroprotective effects in NDs.

3. Conclusion

Looking for dual A_{2A} AR/MAO-B targeted ligands as potential anti-neurodegenerative agents, we have explored the xanthine scaffold with a third heterocyclic ring fused to the *f*-bond and substituted with an (un)substituted aromatic residue. A library of 37 novel compounds was synthesized and biologically evaluated providing an extensive structure-activity relationship analysis for human A_{2A} AR and human MAO-B. Within three investigated series of tricyclic structures, we identified compounds **9p**, **9u**, **10a**, **10e** acting as selective dual A_{2A}/MAO-B ligands with sub-micromolar activity. These structures presenting a dual pharmacological profile may have potential application in PD or AD providing both symptomatic and neuroprotective effects.

Furthermore, the research has resulted in the discovery of selective MAO-B inhibitors **8d**, **9n**, **10d**, **10f** with IC_{50}-values in nanomolar range. The 1,3-dimethylpyrimido[2,1-*f*]purinedione and the 1,3-dimethyldiazepino[2,1-*f*]purinedione scaffolds were in particular suitable for this activity, which was confirmed by molecular docking. The binding mode for these tricyclic structures was slightly shifted as compared to that of the standard inhibitor safinamide, being in close proximity to FAD, and the purinedione core was flipped horizontally and stabilized by π- π stacking.

The *in silico* calculations of selected ADME-Tox parameters predicted hepatotoxicity of all final compounds, however *in vitro* studies provided more insight into the structure-activity relationships. The toxicity may potentially be elevated for the benzyl derivatives of

the tricyclic structures, nevertheless the most active compounds **9n** and **9u** presented low hepatotoxicity when experimentally tested. Therefore, the increased risk of toxic effects seems to be dependent on structural modifications in the aromatic substitutents of the molecule.

Moreover, selected compounds were tested as antioxidants in two different assays. Prevention of lipid peroxidation by tricyclic derivatives based on the xanthine scaffold may indicate additional synergistic neuroprotective effects of the tested compounds, which makes them promising candidates for the treatment of NDs.

4. Experimental protocols

4.1. Chemistry

4.1.1. Material and methods

All commercially available reagents and solvents were used without further purification. Melting points (mp.) were determined on a MEL-TEMP II (LD Inc., USA) melting point apparatus and are uncorrected. ^{1}H NMR spectra were performed with a Varian Mercury-VX 300 MHz PFG spectrometer or a Bruker AMX 300 (Bruker, Germany) spectrometer in DMSO-d_6 or $CDCl_3$ with TMS as an internal standard. Chemical shifts were expressed in parts per million (ppm). ^{13}C NMR data were recorded on 75 MHz on Varian-Mercury-VX 300 MHz PFG or 400 MHz spectrometer. The *J* values are reported in Hertz (Hz), and the splitting patterns are designated as follows: s (singlet), d (doublet), t (triplet), dd (doublet of doublets), dt (doublet of triplets), quin (quintet), m (multiplet). The purity of the final compounds was determined (%) on an Waters TQD mass spectrometer coupled with an Waters ACQUITY UPLC system. Retention times (t_R) are given in minutes. Microwave reactions were performed in CEM Discover System microwave oven. Silica gel 60 (0.063-0.20 mm; Merck) was used for the column chromatography and the mixture of dichloromethane with methanol was applied as a mobile phase. TLC data were obtained using aluminium sheets coated with silica gel 60 F254 (Merck). Eluent system: DCM/MeOH 9:1, DCM/MeOH 9.5:0.5.

The synthesis and physicochemical properties of the compounds **6** and **7a-c** were reported previously.[34,35]

4.1.2. General procedure for the synthesis of imidazo[2,1-*f*]purinedione (8a-f), pyrimido[2,1-*f*]purinedione (9a-v) and diazepino[2,1-*f*]purinedione (10a-i).

A mixture of 0.55 mmol of 8-bromo-7-(2-bromoethyl)theophylline **7a** or 8-bromo-7-(3-chloropropyl)theophylline **7b** or 8-bromo-7-(4-bromobutyl)theophylline **7c**, 1.1 mmol of appropriate aromatic amine, 1,6 mmol of TEBA and 1.00 ml of propanol was heated in closed vessels in microwave oven (300 Watt, Power Max Off, 160 °C, 10 bar) for 1 h. The solvent was removed and the residue was treated with ethanol. The products were purified by crystallization from ethanol or flash column chromatography over silica gel with CH_2Cl_2 : MeOH (100 : 0 to 80 : 20). The precipitate was filtered off and dried.

8-(3-bromobenzyl)-1,3-dimethyl-7,8-dihydro-1*H*-imidazo[2,1-*f*]purine-2,4(3*H*,6*H*)-dione (8a)

Yield: 104 mg; 49 %; mp: 205-207°C; ^{1}H NMR (300 MHz, DMSO-d_6) δ ppm 3.15 (s, 3 H, N3C$\underline{H}_3$), 3.34 (s, 3 H, N1C$\underline{H}_3$), 3.73 - 3.81 (m, 2 H, C7$\underline{H}_2$), 4.05 - 4.13 (m, 2 H, C6$\underline{H}_2$), 4.48

(s, 2 H, N8C$\underline{H}_2$), 7.30 - 7.34 (m, 2 H, C5$\underline{H}$, C6$\underline{H}$, phe), 7.49 - 7.52 (m, 1 H, C2$\underline{H}$), 7.72 - 7.77 (m, 1 H, C4H); UPLC/MS purity 98.3 %; t_R = 5.53; $C_{16}H_{16}BrN_5O_2$; MW 390.23; $[M]^+$ 390.04

8-(3,4-dichlorobenzyl)-1,3-dimethyl-7,8-dihydro-1*H*-imidazo[2,1-*f*]purine-2,4(3*H*,6*H*)-dione (8b)

Yield: 124 mg; 59 %; mp: 202-204°C; ^{1}H NMR (400 MHz, DMSO-d_6) δ ppm 3.19 (br. s., 3 H, N3C$\underline{H}_3$), 3.37 (br. s., 3 H, N1C$\underline{H}_3$), 3.76 - 3.87 (m, 2 H, C7$\underline{H}_2$), 4.06 - 4.19 (m, 2 H, C6$\underline{H}_2$), 4.52 (br. s., 2 H, N8C$\underline{H}_2$), 7.34 - 7.41 (m, 1 H, C6H, phe), 7.62 - 7.69 (m, 2 H, C2H, C5H, phe); UPLC/MS purity 96.7%; t_R = 5.99; $C_{16}H_{15}Cl_2N_5O_2$; MW 380.23; $[M]^+$ 380.07

8-(2-bromobenzyl)-1,3-dimethyl-7,8-dihydro-1*H*-imidazo[2,1-*f*]purine-2,4(3*H*,6*H*)-dione (8c)

Yield: 90 mg; 41 %; mp: 224-226°C; ^{1}H NMR (300 MHz, DMSO-d_6) δ ppm 3.16 (s, 3 H, N3C$\underline{H}_3$), 3.33 (s, 3 H, N1C$\underline{H}_3$), 3.78 - 3.90 (m, 2 H, C7$\underline{H}_2$), 4.08 - 4.18 (m, 2 H, C6$\underline{H}_2$), 4.55 (s, 2 H, N8C$\underline{H}_2$), 7.28 - 7.32 (m, 1 H, C6H, phe), 7.40 (td, *J*=7.62, 1.17 Hz, 1 H, C4H, phe), 7.45 - 7.50 (m, 1 H, C5H, phe), 7.65 (d, *J*=7.03 Hz, 1 H, C3H, phe); ^{13}C NMR (DMSO-d_6) δ ppm 27.8 (N3CH_3), 30.2 (N1CH_3), 43.7 (C6), 50.7 (C7), 52.9 (N8CH_2), 102.5 (C4a), 123.4 (C2, phe), 128.6 (C5, phe), 130.2 (C4, phe), 133.2 (C6, phe), 135.8 (C3, phe), 138.4 (C1, phe), 149.7 (C10a), 151.4 (C2), 152.9 (C4), 160.8 (C9a); UPLC/MS purity 95.8%; t_R = 5.47; $C_{16}H_{16}BrN_5O_2$; MW 390.23; $[M]^+$ 390.04

8-(3-bromo-4-fluorobenzyl)-1,3-dimethyl-7,8-dihydro-1*H*-imidazo[2,1-*f*]purine-2,4(3*H*,6*H*)-dione (8d)

Yield: 116 mg; 52 %; mp: 178-180°C; ^{1}H NMR (400 MHz, CHLOROFORM-*d*) δ ppm: 3.38 (s, 3 H, N3C$\underline{H}_3$), 3.55 (s, 3 H N1C$\underline{H}_3$), 3.77 - 3.84 (m, 2 H, C7$\underline{H}_2$), 4.21 (t, *J*=8.02 Hz, 2 H, C6$\underline{H}_2$), 4.57 (s, 2 H, N8C$\underline{H}_2$), 7.17 - 7.24 (m, 1 H, C3$\underline{H}$, phe), 7.31 - 7.34 (m, 2 H, C5$\underline{H}$,C6H phe); ^{13}C NMR (CHLOROFORM-*d*) δ ppm: 27.8 (N3CH_3), 30.1 (N1CH_3), 43.4 (C6), 43.6 (C7), 52.0 (N8CH_2), 103.0 (C4a), 119.4 (d, $^2J_{C,F}$ = 24.9 Hz, C3, phe), 121.7 (d, $^2J_{C,F}$ = 14.7 Hz, C5, phe), 122.6 (d, $^4J_{C,F}$ = 9.5 Hz, C6, phe), 128.0 (d, $^3J_{C,F}$ = 3.6 Hz, C2, phe), 131.5 (d, $^3J_{C,F}$ = 5.1 Hz, C1, phe), 151.7 (C9a), 153.2 (C8a), 153.8 (C2), 159.5 (C4) 161.2 (d, $^1J_{C,F}$ =176.1 Hz, C4, phe),; UPLC/MS purity 100.0 %; t_R = 5.19; $C_{16}H_{15}BrFN_5O_2$; MW 408.23; $[M+H]^+$ 409.04

8-(4-chlorobenzyl)-1,3-dimethyl-7,8-dihydro-1*H*-imidazo[2,1-*f*]purine-2,4(3*H*,6*H*)-dione (8e)

Yield: 126 mg, 66 %; mp: 216-218°C; ^{1}H NMR (300 MHz, DMSO-d_6) δ ppm 3.16 (s, 3 H, N3C$\underline{H}_3$), 3.34 (br. s., 3 H, N1C$\underline{H}_3$), 3.83 (t, *J*=8.21 Hz, 2 H, C7$\underline{H}_2$), 4.09 - 4.16 (m, 2 H, C6$\underline{H}_2$), 4.58 (s, 2 H, N8C$\underline{H}_2$), 7.33 - 7.38 (m, 2 H, C2H, C6H, phe), 7.46 - 7.52 (m, 2 H, C3H, C5H, phe); ^{13}C NMR (DMSO-d_6) δ ppm 27.8 (N3CH_3), 30.2 (N1CH_3), 43.7 (C6), 48.2 (C7), 52.8 (N8CH_2), 102.5 (C4a), 128.0 (C3, C5, phe), 130.0 (C2, C6, phe), 133.1 (C4, phe), 134.3 (C1, phe), 151.4 (C10a), 153.0 (C2), 153.11 (C4), 160.9 (C9a); UPLC/MS purity 97.2%; t_R = 4.79; $C_{16}H_{16}ClN_5O_2$; MW 345.78; $[M+H]^+$ 346.11

8-(2-methoxybenzyl)-1,3-dimethyl-7,8-dihydro-1*H*-imidazo[2,1-*f*]purine-2,4(3*H*,6*H*)-dione (8f)

Yield: 109 mg; 58 %; mp: 198-200°C; ^{1}H NMR (300 MHz, DMSO-d_6) δ ppm 3.15 (s, 3 H, N3C$\underline{H}_3$), 3.22 - 3.32 (m, 2 H, C7$\underline{H}_2$), 3.33 (s, 3 H, N1C$\underline{H}_3$), 3.78 (s, 3 H, OC$\underline{H}_3$), 3.96 - 4.15 (m, 2 H, C6$\underline{H}_2$), 4.45 (s, 2 H, N9C$\underline{H}_2$), 6.92 (t, *J*=7.03 Hz, 1 H, C4, phe), 7.02 (d, *J*=8.21 Hz, 1 H, C3, phe), 7.18 - 7.37 (m, 2 H, C5, C6, phe); ^{13}C NMR (DMSO-d_6) δ ppm: 27.8 (N3CH_3), 30.2 (N1CH_3), 43.7 (C6), 45.2 (C7), 52.5 (N9CH_2), 55.9 (O$\underline{C}H_3$), 102.3 (C4a), 111.3 (C3,

phe), 112.6 (C5, phe), 115.4 (C1, phe), 120.9 (C4, phe), 124.4 (C6, phe), 129.6 (C10a), 151.4 (C9a), 153.1 (C2), 157.6 (C4), 161.2 (C2, phe); UPLC/MS purity 98.68 %; t_R = 5.21; $C_{17}H_{19}N_5O_3$; MW 341.36; $[M+H]^+$ 342.04

9-(2-Fluorobenzyl)-1,3-dimethyl-6,7,8,9-tetrahydropyrimido[2,1-*f*]purine-2,4(1*H*,3*H*)-dione (9a)

Yield: 136 mg, 72 %; mp: 219 °C; ^{1}H NMR (300 MHz, CHLOROFORM-*d*) δ ppm: 2.13 (dt, *J*=11.73, 5.80 Hz, 2 H, C7$\underline{H}_2$), 3.32 - 3.38 (m, 5 H, N3C$\underline{H}_3$, C8$\underline{H}_2$), 3.55 (s, 3 H, N1C$\underline{H}_3$), 4.22 (t, *J*=6.03 Hz, 2 H, C6$\underline{H}_2$), 4.83 (s, 2 H, N9C$\underline{H}_2$), 7.03 - 7.15 (m, 2 H, C5$\underline{H}$/C6$\underline{H}$, phe), 7.27 - 7.34 (m, 1 H, C3$\underline{H}$, phe), 7.39 - 7.46 (m, 1 H, C4$\underline{H}$, phe). ^{13}C NMR (CHLOROFORM-*d*) δ ppm: 21.4 (C7), 27.6 (N3CH_3), 29.7 (N1CH_3), 41.7 (C6), 44.2 (C8), 46.4 (d, $^3J_{C,F}$ = 4.6 Hz, N9CH_2), 103.0 (C4a), 115.5 (d, $^2J_{C,F}$ = 21.8 Hz, C3, phe), 123.6 (d, $^2J_{C,F}$ = 15 Hz, C1, phe), 124.4 (d, $^4J_{C,F}$ = 3.5 Hz, C5, phe), 129.6 (d, $^3J_{C,F}$ = 8.1 Hz, C4, phe), 130.6 (d, $^3J_{C,F}$ = 4.6 Hz, C6, phe), 148.7 (C10a), 151.6 (C9a), 151.8 (C2), 153.9 (C4), 161.1 (d, $^1J_{C,F}$ =246.4 Hz, C2, phe). UPLC/MS purity 97.01 %, t_R = 5.45. $C_{17}H_{18}FN_5O_2$, MW 343.36, $[M+H]^+$ 344.32.

9-(4-Chloro-3-fluorobenzyl)-1,3-dimethyl-6,7,8,9-tetrahydropyrimido[2,1-*f*]purine-2,4(1*H*,3*H*)-dione (9b)

Yield: 100 mg, 53 %; mp: 196 °C; ^{1}H NMR (300 MHz, CHLOROFORM-*d*) δ ppm: 2.15 (dt, *J*=11.80, 5.90 Hz, 2 H, C7$\underline{H}_2$), 3.27 (t, *J*=5.60 Hz, 2 H, C8$\underline{H}_2$), 3.37 (s, 3 H, N3C$\underline{H}_3$), 3.52 (s, 3 H, N1C$\underline{H}_3$), 4.24 (t, *J*=6.03 Hz, 2 H, C6$\underline{H}_2$), 4.72 (s, 2 H, N9C$\underline{H}_2$), 7.02 - 7.08 (m, 1 H, C2$\underline{H}$, phe), 7.13 (dd, *J*=9.62, 1.92 Hz, 1 H, C6$\underline{H}$, phe), 7.37 (m, *J*=15.64 Hz, 1 H, C5$\underline{H}$, phe). ^{13}C NMR (CHLOROFORM-*d*) δ ppm: 21.4 (C7), 27.6 (N3CH_3), 29.8 (N1CH_3), 41.7 (C6), 44.0 (C8), 52.2 (N9CH_2), 103.1 (C4a), 116.2 (d, $^2J_{C,F}$ = 21.9 Hz, C2, phe), 120.2 (C4, phe), 124.4 (d, $^4J_{C,F}$ = 3.4 Hz, C6, phe), 130.9 (C5, phe), 137.7 (d, $^3J_{C,F}$ = 5.8 Hz, C1, phe), 148.5 (C10a), 151.3 (C9a), 151.8 (C2), 153.9 (C4), 158.2 (d, $^1J_{C,F}$ =249.9 Hz, C3, phe). UPLC/MS purity 97.01 %, t_R = 5.45. $C_{17}H_{18}FN_5O_2$, MW 343.36, $[M+H]^+$ 344.32. UPLC/MS purity 100 %, t_R = 6.13. $C_{17}H_{17}ClFN_5O_2$, MW 377.11, $[M+H]^+$ 378.75.

1,3-Dimethyl-9-(2-(pyridin-3-yl)ethyl)-6,7,8,9-tetrahydropyrimido[2,1-*f*]purine-2,4(1*H*,3*H*)-dione (9c)

Yield: 90 mg, 48 %; mp: 206 °C; ^{1}H NMR (400 MHz, CHLOROFORM-*d*) δ ppm: 2.07 - 2.14 (m, 2 H, C7$\underline{H}_2$), 3.02 (t, *J*=7.24 Hz, 2 H, N9CH_2C$\underline{H}_2$), 3.29 (m, *J*=5.48 Hz, 2 H, C8$\underline{H}_2$), 3.38 (s, 3 H, N3C$\underline{H}_3$), 3.52 (s, 3 H, N1C$\underline{H}_3$), 3.76 - 3.80 (m, 2 H, N9C$\underline{H}_2$), 4.21 (t, *J*=5.87 Hz, 2 H, C6$\underline{H}_2$), 7.31 (dd, *J*=7.63, 4.89 Hz, 1 H, C5$\underline{H}$, pyr), 7.65 (dt, *J*=7.83, 1.76 Hz, 1 H, C6$\underline{H}$, pyr), 8.51 (dd, *J*=4.69, 1.57 Hz, 1 H, C4$\underline{H}$, pyr), 8.54 - 8.56 (m, 1 H, C2$\underline{H}$, pyr). ^{13}C NMR (CHLOROFORM-*d*) δ ppm: 21.4 (C7), 27.6 (N3CH_3), 29.7 (N1CH_3), 31.2, (N9$CH_2\underline{C}H_2$), 41.6 (C6), 45.4 (C8), 51.0 (N9$\underline{C}H_2CH_2$), 102.9 (C4a), 123.7 (C5, pyr), 134.8 (C6, pyr), 137.2 (C1, pyr), 147.2 (C4, pyr), 148.9 (C10a), 149.3 (C2, pyr), 151.9 (C2), 153.9 (C4). UPLC/MS purity 95.07 %, t_R = 2.34. $C_{17}H_{20}N_6O_2$, MW 340.39, $[M+H]^+$ 341.13.

9-(2-Chloro-4-fluorobenzyl)-1,3-dimethyl-6,7,8,9-tetrahydropyrimido[2,1-*f*]purine-2,4(1*H*,3*H*)-dione (9d)

Yield: 75 mg, 36 %; mp: 190 °C; ^{1}H NMR (400 MHz, CHLOROFORM-*d*) δ ppm: 2.14 - 2.21 (m, 2 H, C7$\underline{H}_2$), 3.35 (t, *J*=5.90 Hz, 2 H, C8$\underline{H}_2$), 3.39 (s, 3 H, N3C$\underline{H}_3$), 3.56 (s, 3 H, N1C$\underline{H}_3$), 4.27 (t, *J*=6.06 Hz, 2 H, C6$\underline{H}_2$), 4.90 (s, 2 H, N9C$\underline{H}_2$), 7.00 (td, *J*=8.31, 2.54 Hz, 1 H, C5$\underline{H}$, phe), 7.18 (m, *J*=2.74 Hz, 1 H, C6$\underline{H}$, phe), 7.43 (dd, *J*=8.61, 5.87 Hz, 1 H, C3$\underline{H}$, phe). ^{13}C NMR (CHLOROFORM-*d*) δ ppm: 21.4 (C7), 27.7 (N3CH_3), 30.0 (N1CH_3), 41.7 (C6), 44.4 (C8), 49.9 (N9CH_2), 103.0 (C4a), 114.5 (d, $^2J_{C,F}$ = 20.5 Hz, C5, phe), 117.2 (d,

$^{2}J_{C,F}$ = 25 Hz, C3, phe), 130.1 (d, $^{4}J_{C,F}$ = 3.7 Hz, C1, phe) , 131.1 (d, $^{3}J_{C,F}$ = 8.8 Hz, C6, phe), 134.5 (d, $^{3}J_{C,F}$ = 10.3 Hz, C2, phe), 148.1 (C10a), 151.1 (C9a), 151.8 (C2), 153.9 (C4), 162.0 (d, $^{1}J_{C,F}$ =250.1 Hz, C4, phe). UPLC/MS purity 98.18 %, t_R = 6.18. $C_{17}H_{17}ClFN_5O_2$, MW 377.80, $[M+H]^+$ 378.29.

9-(3-Bromo-4-fluorobenzyl)-1,3-dimethyl-6,7,8,9-tetrahydropyrimido[2,1-*f*]purine-2,4(1*H*,3*H*)-dione (9e)

Yield: 70 mg, 30 %; mp: 199 °C; ^{1}H NMR (400 MHz, CHLOROFORM-*d*) δ ppm: 2.16 (quin, *J*=5.87 Hz, 2 H, C7$\underline{H}_2$), 3.28 (t, *J*=5.50 Hz, 2 H, C8$\underline{H}_2$), 3.39 (s, 3 H, N3C$\underline{H}_3$), 3.55 (s, 3 H, N1C$\underline{H}_3$), 4.25 (t, *J*=6.06 Hz, 2 H, C6$\underline{H}_2$), 4.71 (s, 2 H, N9C$\underline{H}_2$), 7.11 (t, *J*=8.41 Hz, 1 H, C5$\underline{H}$, phe), 7.25 - 7.28 (m, 1 H, C6$\underline{H}$, phe), 7.55 (dd, *J*=6.46, 2.15 Hz, 1 H, C2$\underline{H}$, phe). ^{13}C NMR (CHLOROFORM-*d*) δ ppm: 21.4 (C7), 27.7 ($N3CH_3$), 29.8 ($N1CH_3$), 41.7 (C6), 44.0 (C8), 52.0 ($N9CH_2$), 103.1 (C4a), 109.4 (d, $^{2}J_{C,F}$ = 21.2 Hz, C3, phe), 116.7 (d, $^{2}J_{C,F}$ = 22 Hz, C5, phe), 128.7 (d, $^{3}J_{C,F}$ = 7.4 Hz, C6, phe), 133.2 (C2, phe), 134.1 (d, $^{4}J_{C,F}$ = 3.7 Hz, C1, phe), 148.5 (C10a), 151.3 (C9a), 151.8 (C2), 153.9 (C4), 158.7 (d, $^{1}J_{C,F}$ = 248 Hz, C4, phe). UPLC/MS purity 100 %, t_R = 6.23. $C_{17}H_{17}BrFN_5O_2$, MW 422.26, $[M+H]^+$ 422.01.

1,3-Dimethyl-9-(3,4,5-trifluorobenzyl)-6,7,8,9-tetrahydropyrimido[2,1-*f*]purine-2,4(1*H*,3*H*)-dione (9f)

Yield: 95 mg, 46 %; mp: 236 °C; ^{1}H NMR (400 MHz, CHLOROFORM-*d*) δ ppm: 2.16 - 2.23 (m, 2 H, C7$\underline{H}_2$), 3.31 (t, *J*=5.90 Hz, 2 H, C8$\underline{H}_2$), 3.39 (s, 3 H, N3C$\underline{H}_3$), 3.54 (s, 3 H, N1C$\underline{H}_3$), 4.27 (t, *J*=6.06 Hz, 2 H, C6$\underline{H}_2$), 4.71 (s, 2 H, N9C$\underline{H}_2$), 6.96 - 7.02 (m, 2 H, C2$\underline{H}$/C6$\underline{H}$, phe). ^{13}C NMR (CHLOROFORM-*d*) δ ppm: 21.4 (C7), 27.7 ($N3CH_3$), 29.9 ($N1CH_3$), 41.7 (C6), 44.2 (C8), 52.3 ($N9CH_2$), 103.2 (C4a), 111.8-112.1 (m, C2/C6, phe), 133.0-133.2 (m, C1, phe), 140.6 (C4, phe), 148.2 (C10a), 151.0 (C9a), 151.8 (C2), 152.6 (dd, $^{3}J_{C,F}$ = 10.3, $^{4}J_{C,F}$ = 3.7 Hz, C3/C5, phe), 154.0 (C4). UPLC/MS purity 100 %, t_R = 5.93. $C_{17}H_{16}F_3N_5O_2$, MW 379.34, $[M+H]^+$ 380.35.

1,3-Dimethyl-9-(thiophen-2-ylmethyl)-6,7,8,9-tetrahydropyrimido[2,1-*f*]purine-2,4(1H,3H)-dione (9g)

Yield: 75 g, 41 %; mp: 203 °C; ^{1}H NMR (300 MHz, CHLOROFORM-*d*) δ ppm: 2.13 (dt, *J*=11.72, 5.86 Hz, 2 H, C7$\underline{H}_2$), 3.28 - 3.33 (m, 2 H, C8$\underline{H}_2$), 3.35 (s, 3 H, N3C$\underline{H}_3$), 3.53 (s, 3 H, N1C$\underline{H}_3$), 4.19 (t, *J*=6.15 Hz, 2 H, C6$\underline{H}_2$), 4.87 (s, 2 H, N9C$\underline{H}_2$), 6.95 (dd, *J*=4.69, 3.52 Hz, 1 H, C4$\underline{H}$, thiophen-2-yl), 7.00 - 7.03 (m, 1 H, C5$\underline{H}$, thiophen-2-yl), 7.23 (dd, *J*=4.69, 1.17 Hz, 1 H, C3$\underline{H}$, thiophen-2-yl).^{13}C NMR (CHLOROFORM-*d*) δ ppm: 21.4 (C7), 27.6 ($N3CH_3$), 29.7 ($N1CH_3$), 41.7 (C6), 43.7 (C8), 47.7 ($N9CH_2$), 103.1 (C4a), 125.7 (C5, thiophen-2-yl), 126.77 (C3/C4, thiophen-2-yl), 138.8 (C2, thiophen-2-yl), 148.8 (C10a), 151.3 (C9a), 151.9 (C2), 153.9 (C4). UPLC/MS purity 94.72 %, t_R = 5.08. $C_{15}H_{17}N_5O_2S$, MW 331.39, $[M+H]^+$ 332.28.

9-(5-Bromo-2-fluorobenzyl)-1,3-dimethyl-6,7,8,9-tetrahydropyrimido[2,1-*f*]purine-2,4(1*H*,3*H*)-dione (9h)

Yield: 88 mg, 38 %; mp: 194 °C; ^{1}H NMR (400 MHz, CHLOROFORM-*d*) δ ppm: 2.18 (dt, *J*=11.74, 5.87 Hz, 2 H, C7$\underline{H}_2$), 3.35 - 3.40 (m, 5 H, C8$\underline{H}_2$, N3C$\underline{H}_3$), 3.57 (s, 3 H, N1C$\underline{H}_3$), 4.25 (t, *J*=6.06 Hz, 2 H, C6$\underline{H}_2$), 4.79 (s, 2 H, N9C$\underline{H}_2$), 6.96 - 7.02 (m, 1 H, C3$\underline{H}$, phe), 7.39 - 7.44 (m, 1 H, C6$\underline{H}$, phe), 7.60 (dd, $J_{H,F}$=6.46, 2.54 Hz, 1 H, C4, phe). ^{13}C NMR (CHLOROFORM-*d*) δ ppm: 21.4 (C7), 27.7 ($N3CH_3$), 29.9 ($N1CH_3$), 41.7 (C6), 44.6 (C8), 46.5 ($N9CH_2$), 103.1 (C4a), 116.9 (C5, phe), 117.3 (d, $^{2}J_{C,F}$ = 23.5 Hz, C3, phe), 125.9 (d, $^{2}J_{C,F}$ = 16.9 Hz, C1, phe), 132.5 (d, $^{3}J_{C,F}$ = 8.07 Hz, C4, phe), 133.6 (d, $^{3}J_{C,F}$ = 4.4 Hz, C6, phe), 148.2 (C10a), 151.0

(C9a), 151.8 (C2), 154.0 (C4), 161.2 (d, $^{1}J_{C,F}$ = 247.3 Hz, C2, phe). UPLC/MS purity 98.40 %, t_R = 6.25. $C_{17}H_{17}BrFN_5O_2$, MW 422.26, $[M+H]^+$ 424.01.

1,3-Dimethyl-9-(2-(pyridin-4-yl)ethyl)-6,7,8,9-tetrahydropyrimido[2,1-*f*]purine-2,4(1*H*,3*H*)-dione (9i)

Yield: 40 mg, 21 %; mp: 205 °C; ^{1}H NMR (400 MHz, CHLOROFORM-*d*) δ ppm: 2.10 (dt, *J*=11.74, 5.87 Hz, 2 H, C7H$_2$), 3.03 (t, *J*=7.24 Hz, 2 H, N9CH$_2$CH$_2$), 3.28 (t, *J*=5.90 Hz, 2 H, C8H$_2$), 3.38 (s, 3 H, N3CH$_3$), 3.53 (s, 3 H, N1CH$_3$), 3.80 (t, *J*=7.40 Hz, 2 H, N9CH$_2$), 4.21 (t, *J*=6.06 Hz, 2 H, C6H$_2$), 7.25 - 7.28 (m, 2 H, C2H/ C6H, pyr), 8.55 - 8.58 (m, 2 H, C3H/ C5H, pyr). ^{13}C NMR (CHLOROFORM-*d*) δ ppm: 21.4 (C7), 27.6 (N3CH$_3$), 29.7 (N1CH$_3$), 33.5 (N9CH$_2$CH$_2$), 41.6 (C6), 45.5 (C8), 50.4 (N9CH$_2$CH$_2$), 103.0 (C4a), 124.5 (C2/C6, pyr), 148.7 (C10a), 148.9 (C1, pyr), 149.3 (C3/5, pyr), 151.1 (C9a), 151,9 (C2), 153.9 (C4). UPLC/MS purity 96.37 %, t_R = 2.30, $C_{17}H_{20}N_6O_2$, MW 340.39, $[M+H]^+$ 341.13.

9-(3-Chloro-4-methoxybenzyl)-1,3-dimethyl-6,7,8,9-tetrahydropyrimido[2,1-*f*]purine-2,4(1*H*,3*H*)-dione (9j)

Yield: 88 mg, 41 %; mp: 213 °C; ^{1}H NMR (300 MHz, CHLOROFORM-*d*) δ ppm: 2.11 (quin, *J*=5.86 Hz, 2 H, C7H$_2$), 3.23 (t, *J*=5.30 Hz, 2 H, C8H$_2$), 3.36 (s, 3 H, N3CH$_3$), 3.52 (s, 3 H, N1CH$_3$), 3.89 (s, 3 H, OCH$_3$), 4.21 (t, *J*=5.86 Hz, 2 H, C6H$_2$), 4.64 (s, 2 H, N9CH$_2$), 6.89 (d, *J*=8.21 Hz, 1 H, C5H, phe), 7.18 (dd, *J*=8.50, 2.05 Hz, 1 H, C6H, phe), 7.33 (d, *J*=2.34 Hz, 1 H, C2H, phe). ^{13}C NMR (CHLOROFORM-*d*) δ ppm: 21.4 (C7), 27.6 (N3CH$_3$), 29.7 (N1CH$_3$), 41.6 (C6), 43.6 (C8), 52.0 (N9CH$_2$), 56.2 (OCH$_3$), 103.0 (C4a), 112.1 (C5, phe), 122.6 (C3, phe), 127.6 (C2, phe), 129.7 (C6, phe), 130.1 (C1, phe), 148.8 (C10a), 151.6 (C9a), 151,9 (C2), 153.9 (C4), 154.6 (C4, phe). UPLC/MS purity 95.94 %, t_R = 5.77, $C_{18}H_{20}ClN_5O_3$, MW 389.84, $[M+H]^+$ 390.04.

9-(4-Chloro-2-fluorobenzyl)-1,3-dimethyl-6,7,8,9-tetrahydropyrimido[2,1-*f*]purine-2,4(1*H*,3*H*)-dione (9k)

Yield: 72 mg, 35 %; mp: 192 °C; ^{1}H NMR (300 MHz, CHLOROFORM-*d*) δ ppm: 2.14 (dt, *J*=11.72, 5.86 Hz, 2 H, C7H$_2$), 3.30 - 3.37 (m, 5 H, C8H$_2$, N3CH$_3$), 3.51 (s, 3 H, N1CH$_3$), 4.21 (t, *J*=6.15 Hz, 2 H, C6H$_2$), 4.74 (s, 2 H, N9CH$_2$), 7.11 (d, *J*=8.79 Hz, 2 H, C5H/C6H, phe), 7.37 (m, *J*=15.82 Hz, 1 H, C3H, phe). ^{13}C NMR (CHLOROFORM-*d*) δ ppm: 21.4 (C7), 27.6 (N3CH$_3$), 29.7 (N1CH$_3$), 41.7 (C6), 44.4 (C8), 46.1 (N9CH$_2$), 103.1 (C4a), 116.3 (d, $^{2}J_{C,F}$ = 25.5 Hz, C3, phe), 122.5 (C1, phe), 124.9 (d, $^{4}J_{C,F}$ = 3.5 Hz, C5, phe), 131.5 (d, $^{3}J_{C,F}$ = 4.6 Hz, C6, phe), 134.5 (d, $^{3}J_{C,F}$ = 10.4 Hz, C4, phe), 148.6 (C10a), 151.4 (C9a), 151.8 (C2), 153.9 (C4), 159.2 (C2, phe). UPLC/MS purity 100 %, t_R = 6.30, $C_{17}H_{17}ClFN_5O_2$, MW 377.80, $[M+H]^+$ 378.01.

9-(4-Bromo-2-fluorobenzyl)-1,3-dimethyl-6,7,8,9-tetrahydropyrimido[2,1-*f*]purine-2,4(1*H*,3*H*)-dione (9l)

Yield: 94 mg, 40 %; mp: 203 °C; ^{1}H NMR (300 MHz, CHLOROFORM-*d*) δ ppm: 2.09 - 2.18 (m, 2 H, C7H$_2$), 3.30 - 3.37 (m, 5 H, C8H$_2$, N3CH$_3$), 3.51 (s, 3 H, N1CH$_3$), 4.21 (t, *J*=5.86 Hz, 2 H, C6H$_2$), 4.72 (s, 2 H, N9CH$_2$), 7.23 - 7.35 (m, 3 H, C3H/C5H/C6H, phe). ^{13}C NMR (CHLOROFORM-*d*) δ ppm: 21.4 (C7), 27.6 (N3CH$_3$), 29.7 (N1CH$_3$), 41.7 (C6), 44.4 (C8), 46.4 (N9CH$_2$), 103.1 (C4a), 119.2 (d, $^{2}J_{C,F}$ = 25.3 Hz, C3, phe), 122.0 (d, $^{3}J_{C,F}$ = 10.8 Hz, C4, phe), 122.9 (d, $^{2}J_{C,F}$ = 16.1 Hz, C1, phe), 127.8 (d, $^{4}J_{C,F}$ = 4.6 Hz, C5, phe), 131.8 (d, $^{3}J_{C,F}$ = 4.6 Hz, C6, phe), 148.7 (C10a), 151.4 (C9a), 151,8 (C2), 153.9 (C4), 159.9 (d, $^{1}J_{C,F}$ = 251 Hz, C2, phe). UPLC/MS purity 100 %, t_R = 6.47, $C_{17}H_{17}BrFN_5O_2$, MW 422.26, $[M+H]^+$ 423.94.

9-(3-Bromobenzyl)-1,3-dimethyl-6,7,8,9-tetrahydropyrimido[2,1-*f*]purine-2,4(1*H*,3*H*)-dione (9m)

Yield: 96 mg, 43 %; mp: 162 °C; ^{1}H NMR (300 MHz, DMSO-d_6) δ ppm: 2.05 (quin, *J*=5.71 Hz, 2 H, C7$\underline{H}_2$), 3.15 (s, 3 H, N3C$\underline{H}_3$), 3.25 - 3.30 (m, 2 H, C8$\underline{H}_2$), 3.32 (s, 3 H, N1C$\underline{H}_3$), 4.06 (t, *J*=5.86 Hz, 2 H, C6$\underline{H}_2$), 4.67 (s, 2 H, N9C$\underline{H}_2$), 7.26 - 7.35 (m, 2 H, C5$\underline{H}$/C6$\underline{H}$, phe), 7.44 - 7.49 (m, 1 H, C2$\underline{H}$, phe), 7.52 - 7.54 (m, 1 H, C4$\underline{H}$, phe). ^{13}C NMR (DMSO-d_6) δ ppm: 21.2 (C7), 27.6 (N3CH_3), 29.8 (N1CH_3), 41.8 (C6), 44.2 (C8), 51.9 (N9CH_2), 102.6 (C4a), 122.3 (C3, phe), 127.2 (C6, phe), 130.7 (C5, phe), 130.9 (C4, phe), 131.2 (C2, phe), 140.5 (C1, phe), 148.5 (C10a), 151.4 (C9a), 151.8 (C2), 153.1 (C4). UPLC/MS purity 98.96 %, t_R = 6.19, $C_{17}H_{18}BrN_5O_2$, MW 404.27, $[M+H]^+$ 406.99.

9-(2-Bromobenzyl)-1,3-dimethyl-6,7,8,9-tetrahydropyrimido[2,1-*f*]purine-2,4(1*H*,3*H*)-dione (9n)

Yield: 99 mg, 45 %; mp: 194 °C; ^{1}H NMR (300 MHz, CHLOROFORM-*d*) δ ppm: 2.16 (dt, *J*=11.72, 5.86 Hz, 2 H, C7$\underline{H}_2$), 3.30 - 3.37 (m, 5 H, N3C$\underline{H}_3$, C8$\underline{H}_2$), 3.49 (s, 3 H, N1C$\underline{H}_3$), 4.25 (t, *J*=6.15 Hz, 2 H, C6$\underline{H}_2$), 4.86 (s, 2 H, N9C$\underline{H}_2$), 7.13 - 7.20 (m, 1 H, C4$\underline{H}$, phe), 7.28 - 7.36 (m, 2 H, C5$\underline{H}$/C6$\underline{H}$, phe), 7.55 - 7.60 (m, 1 H, C3$\underline{H}$, phe). ^{13}C NMR (CHLOROFORM-*d*) δ ppm: 21.5 (C7), 27.6 (N3CH_3), 29.8 (N1CH_3), 41.7 (C6), 44.3 (C8), 53.0 (N9CH_2), 103.1 (C4a), 123.7 (C2, phe), 127.8 (C5, phe), 129.2 (C4, phe), 129.3 (C6, phe), 133.1 (C3, phe), 135.8 (C1, phe), 148.8 (C10a), 151.7 (C9a), 151,9 (C2), 153.8 (C4). UPLC/MS purity 98.21 %, t_R = 6.19, $C_{17}H_{18}BrN_5O_2$, MW 404.27, $[M+H]^+$ 406.00.

9-(4-Chloro-3-(trifluoromethyl)benzyl)-1,3-dimethyl-6,7,8,9-tetrahydropyrimido[2,1-*f*]purine-2,4(1*H*,3*H*)-dione (9o)

Yield: 69 mg, 29 %; mp: 185 °C; ^{1}H NMR (300 MHz, CHLOROFORM-*d*) δ ppm: 2.16 (dt, *J*=11.72, 5.86 Hz, 2 H, C7$\underline{H}_2$), 3.28 (t, *J*=5.90 Hz, 2 H, C8$\underline{H}_2$), 3.36 (s, 3 H, N3C$\underline{H}_3$), 3.50 (s, 3 H, N1C$\underline{H}_3$), 4.24 (t, *J*=6.15 Hz, 2 H, C6$\underline{H}_2$), 4.73 (s, 2 H, N9C$\underline{H}_2$), 7.42 - 7.51 (m, 2 H, C5$\underline{H}$/C6$\underline{H}$, phe), 7.66 - 7.69 (m, 1 H, C2$\underline{H}$, phe). ^{13}C NMR (CHLOROFORM-*d*) δ ppm: 21.4 (C7), 27.6 (N3CH_3), 29.7 (N1CH_3), 41.7 (C6), 44.2 (C8), 52.2 (N9CH_2), 103.2 (C4a), 120.8 ($\underline{C}F_3$), 127.3-127.4 (m, C2, phe), 128.5 (C3, phe), 131.9 (C5, phe), 132.4 (C4/6, phe), 136.0 (C1, phe), 148.6 (C10a), 151.3 (C9a), 151,8 (C2), 154.0 (C4). UPLC/MS purity 96.35 %, t_R = 6.80, $C_{18}H_{17}ClF_3N_5O_2$, MW 427.81, $[M+H]^+$ 428.06.

9-(6-Chloro-2-fluoro-3-methoxybenzyl)-1,3-dimethyl-6,7,8,9-tetrahydropyrimido[2,1-*f*]purine-2,4(1*H*,3*H*)-dione (9p)

Yield: 78 mg, 35 %; mp: 193 °C; ^{1}H NMR (300 MHz, CHLOROFORM-*d*) δ ppm: 2.04 - 2.12 (m, 2 H, C7$\underline{H}_2$), 3.23 (t, *J*=5.90 Hz, 2 H, C8$\underline{H}_2$), 3.35 (s, 3 H, N3C$\underline{H}_3$), 3.52 (s, 3 H, N1C$\underline{H}_3$), 3.88 (s, 3 H OC$\underline{H}_3$), 4.19 (t, *J*=6.15 Hz, 2 H, C6$\underline{H}_2$), 4.92 (d, *J*=1.76 Hz, 2 H, N9C$\underline{H}_2$), 6.89 (t, *J*=9.08 Hz, 1 H, C4$\underline{H}$, phe), 7.15 (dd, *J*=8.79, 1.76 Hz, 1 H, C5$\underline{H}$, phe). ^{13}C NMR (CHLOROFORM-*d*) δ ppm: 21.4 (C7), 27.6 (N3CH_3), 29.7 (N1CH_3), 41.6 (C6), 43.4 (O$\underline{C}H_3$), 44.3 (C8), 56.4 (N9CH_2), 103.0 (C4a), 113.5 (d, $^{3}J_{C,F}$ = 2.3 Hz, C4, phe), 122.3 (d, $^{2}J_{C,F}$ = 13.8 Hz, C1, phe), 124.8 (d, $^{3}J_{C,F}$ = 4.6 Hz, C6, phe), 126.5 (d, $^{4}J_{C,F}$ = 4.6 Hz, C5, phe), 146.8 (d, $^{2}J_{C,F}$ = 11.5 Hz, C3, phe), 148.6 (C10a), 151.3 (C9a), 151,8 (C2), 153.6 (C2, phe), 154.0 (C4). UPLC/MS purity 97.77 %, t_R = 5.87, $C_{18}H_{19}ClFN_5O_3$, MW 407.83, $[M+H]^+$ 407.99.

9-(2-Chloro-5-(trifluoromethyl)benzyl)-1,3-dimethyl-6,7,8,9-tetrahydropyrimido[2,1-f]purine-2,4(1H,3H)-dione (9q)

Yield: 85 mg, 36 %; mp: 215 °C; ^{1}H NMR (300 MHz, CHLOROFORM-*d*) δ ppm: 2.19 (quin, *J*=5.86 Hz, 2 H, C7$\underline{H}_2$), 3.36 (s, 3 H, N3C$\underline{H}_3$), 3.41 (t, *J*=5.90 Hz, 2 H, C8$\underline{H}_2$), 3.49 (s, 3 H,

N1C$\underline{H}_3$), 4.26 (t, *J*=5.86 Hz, 2 H, C6$\underline{H}_2$), 4.86 (s, 2 H, N9C$\underline{H}_2$), 7.50 - 7.53 (m, 2 H, C3$\underline{H}$/C4$\underline{H}$, phe), 7.73 - 7.76 (m, 1 H, C6$\underline{H}$, phe). ^{13}C NMR (CHLOROFORM-*d*) δ ppm: 21.5 (C7), 27.6 (N3CH_3), 29.7 (N1CH_3), 41.7 (C6), 45.2 (C8), 50.6 (N9CH_2), 103.2 (C4a), 125.8 (d, $^3J_{C,F}$ = 3.5 Hz, C4, phe), 127.1 (d, $^3J_{C,F}$ = 2.5 Hz, C6, phe), 129.7 (C5, phe), 130.3 (C3, phe), 135.6 (C1, phe), 137.5 (C2, phe), 148.8 (C10a), 151.7 (C9a), 151,9 (C2), 154.0 (C4). UPLC/MS purity 100 %, t_R = 6.80, $C_{18}H_{17}ClF_3N_5O_2$, MW 427.81, $[M+H]^+$ 428.06.

9-(4-(*tert*-Butyl)benzyl)-1,3-dimethyl-6,7,8,9-tetrahydropyrimido[2,1-*f*]purine-2,4(1*H*,3*H*)-dione (9r)

Yield: 93 mg, 40 %; mp: 178 °C; ^{1}H NMR (300 MHz, CHLOROFORM-*d*) δ ppm: 1.31 (s, 9 H, C(C$\underline{H}_3$)$_2$), 2.11 (dt, *J*=11.72, 5.86 Hz, 2 H, C7$\underline{H}_2$), 3.26 (t, *J*=5.30 Hz, 2 H, C8$\underline{H}_2$), 3.37 (s, 3 H, N3C$\underline{H}_3$), 3.52 (s, 3 H, N1C$\underline{H}_3$), 4.21 (t, *J*=5.86 Hz, 2 H, C6$\underline{H}_2$), 4.71 (s, 2 H, N9C$\underline{H}_2$), 7.20 - 7.25 (m, 2 H, C2$\underline{H}$/C6$\underline{H}$, phe), 7.33 - 7.38 (m, 2 H, C3$\underline{H}$/C5$\underline{H}$, phe). ^{13}C NMR (CHLOROFORM-*d*) δ ppm: 21.3 (C7), 27.6 (N3CH_3), 29.7 (N1CH_3), 31.3 (C(C$\underline{H}_3$)$_3$), 34.5 (C(CH_3)$_3$), 41.7 (C6), 43.7 (C8), 52.6 (N9CH_2), 103.0 (C4a), 125.6 (C3/5, phe), 126.0 (C2/6, phe), 127.7 (C1, phe), 133.5 (C4, phe), 148.9 (C10a), 150.8 (C9a), 151,9 (C2), 153.9 (C4). UPLC/MS purity 100 %, t_R = 7.38, $C_{21}H_{27}N_5O_2$, MW 427.81, $[M+H]^+$ 382.20.

1,3-Dimethyl-9-(2-methylbenzyl)-6,7,8,9-tetrahydropyrimido[2,1-*f*]purine-2,4(1*H*,3*H*)-dione (9s)

Yield: 101 mg, 54 %; mp: 222 °C; ^{1}H NMR (300 MHz, CHLOROFORM-*d*) δ ppm: 2.06 - 2.17 (m, 2 H, C7$\underline{H}_2$), 2.33 (s, 3 H, C$\underline{H}_3$), 3.20 (t, *J*=5.90 Hz, 2 H, C8$\underline{H}_2$), 3.37 (s, 3 H, N3C$\underline{H}_3$), 3.50 (s, 3 H, N1C$\underline{H}_3$), 4.24 (t, *J*=6.15 Hz, 2 H, C6$\underline{H}_2$), 4.75 (s, 2 H, N9C$\underline{H}_2$), 7.16 - 7.24 (m, 4 H, C3$\underline{H}$/C4$\underline{H}$/C5$\underline{H}$/C6$\underline{H}$, phe). ^{13}C NMR (CHLOROFORM-*d*) δ ppm: 19.2 (CH_3), 21.4 (C7), 27.6 (N3CH_3), 29.7 (N1CH_3), 41.7 (C6), 43.4 (C8), 50.8 (N9CH_2), 103.0 (C4a), 126.1 (C5, phe), 127.8 (C4, phe), 128.5 (C6, phe), 130.7 (C2, phe), 134.2 (C1, phe), 136.8 (C4, phe), 148.9 (C10a), 151.9 (C9a), 151,9 (C2), 153.9 (C4). UPLC/MS purity 98.46 %, t_R = 5.86, $C_{18}H_{21}N_5O_2$, MW 339.40, $[M+H]^+$ 340.20.

1,3-Dimethyl-9-(3-methylbenzyl)-6,7,8,9-tetrahydropyrimido[2,1-*f*]purine-2,4(1*H*,3*H*)-dione (9t)

Yield: 97 mg, 52 %; mp: 171 °C; ^{1}H NMR (300 MHz, CHLOROFORM-*d*) δ ppm: 2.11 (dt, *J*=11.72, 5.86 Hz, 2 H, C7$\underline{H}_2$), 2.34 (s, 3 H, C$\underline{H}_3$), 3.24 (t, *J*=5.90 Hz, 2 H, C8$\underline{H}_2$), 3.37 (s, 3 H, N3C$\underline{H}_3$), 3.53 (s, 3 H, N1C$\underline{H}_3$), 4.22 (t, *J*=6.15 Hz, 2 H, C6$\underline{H}_2$), 4.71 (s, 2 H, N9C$\underline{H}_2$), 7.07 - 7.14 (m, 3 H, C2$\underline{H}$/C4$\underline{H}$/C6$\underline{H}$, phe), 7.19 - 7.24 (m, 1 H, C5$\underline{H}$, phe). ^{13}C NMR (CHLOROFORM-*d*) δ ppm: 21.3 (C7), 21.4 (CH_3), 27.6 (N3CH_3), 29.8 (N1CH_3), 41.7 (C6), 43.6 (C8), 52.9 (N9CH_2), 102.9 (C4a), 125.1 (C6, phe), 128.6 (C4, phe), 128.6 (C5, phe), 128.8 (C2, phe), 136.5 (C1, phe), 138.4 (C3, phe), 148.8 (C10a), 151.8 (C9a), 151,9 (C2), 153.9 (C4). UPLC/MS purity 99.11 %, t_R = 5.94, $C_{18}H_{21}N_5O_2$, MW 339.40, $[M+H]^+$ 340.20.

9-(2-Chloro-6-fluorobenzyl)-1,3-dimethyl-6,7,8,9-tetrahydropyrimido[2,1-*f*]purine-2,4(1*H*,3*H*)-dione (9u)

Yield: 88 mg, 42 %; mp: 236 °C; ^{1}H NMR (300 MHz, CHLOROFORM-*d*) δ ppm: 2.08 (quin, *J*=5.86 Hz, 2 H, C7$\underline{H}_2$), 3.23 (t, *J*=5.90 Hz, 2 H, C8$\underline{H}_2$), 3.35 (s, 3 H, N3C$\underline{H}_3$), 3.51 (s, 3 H, N1C$\underline{H}_3$), 4.19 (t, *J*=5.86 Hz, 2 H, C6$\underline{H}_2$), 4.92 (d, *J*=1.76 Hz, 2 H, N9C$\underline{H}_2$), 6.98 - 7.06 (m, 1 H, C4$\underline{H}$, phe), 7.22 - 7.28 (m, 2 H, C3$\underline{H}$/C5$\underline{H}$, phe). ^{13}C NMR (CHLOROFORM-*d*) δ ppm: 21.4 (C7), 27.6 (N3CH_3), 29.7 (N1CH_3), 41.6 (C6), 43.4 (C8), 44.0 (d, $^3J_{C,F}$ = 3.4 Hz, N9CH_2), 103.0 (C4a), 114.3 (d, $^2J_{C,F}$ = 21.9 Hz, C5, phe), 121.9 (d, $^2J_{C,F}$ = 17.2 Hz, C1, phe), 125.7 (d, $^4J_{C,F}$ = 3.5 Hz, C3, phe), 130.0 (d, $^3J_{C,F}$ = 10.4 Hz, C4, phe), 136.2 (d, $^3J_{C,F}$ = 5.8 Hz,

C2, phe), 148.8 (C10a), 151.4 (C9a), 151,9 (C2), 154.0 (C4), 162.3 (d, $^{1}J_{C,F}$ = 245.0 Hz, C6, phe). UPLC/MS purity 98.32 %, t_R = 5.92, $C_{17}H_{17}ClFN_5O_2$, MW 377.80, $[M+H]^+$ 378.08.

9-(2,5-Dichlorobenzyl)-1,3-dimethyl-6,7,8,9-tetrahydropyrimido[2,1-*f*]purine-2,4(1*H*,3*H*)-dione (9v)

Yield: 79 mg, 36 %; mp: 174 °C; ^{1}H NMR (300 MHz, CHLOROFORM-*d*) δ ppm: 2.14 - 2.23 (m, 2 H, C7$\underline{H}_2$), 3.33 - 3.38 (m, 5 H, C8$\underline{H}_2$, N3C$\underline{H}_3$), 3.49 (s, 3 H, N1C$\underline{H}_3$), 4.26 (t, *J*=6.15 Hz, 2 H, C6$\underline{H}_2$), 4.81 (s, 2 H, N9C$\underline{H}_2$), 7.19 - 7.24 (m, 1 H, C3$\underline{H}$, phe), 7.30 - 7.38 (m, 2 H, C4$\underline{H}$/C6$\underline{H}$, phe). ^{13}C NMR (CHLOROFORM-*d*) δ ppm: 21.5 (C7), 27.6 (N3CH_3), 29.7 (N1CH_3), 41.7 (C6), 44.7 (C8), 50.3 (N9CH_2), 103.2 (C4a), 129.0 (C4, phe), 129.4 (C6, phe), 130.8 (C3, phe), 131.8 (C2, phe), 133.0 (C5, phe), 136.2 (C1, phe), 148.7 (C10a), 151.5 (C9a), 151,8 (C2), 154.0 (C4). UPLC/MS purity 99.31 %, t_R = 6.59, $C_{17}H_{17}Cl_2N_5O_2$, MW 394.26, $[M+H]^+$ 394.03.

10-(2-chlorobenzyl)-1,3-dimethyl-7,8,9,10-tetrahydro-1*H*-[1,3]diazepino[2,1-*f*]purine-2,4(3*H*,6*H*)-dione (10a)

Yield: 156 mg; 76 %; mp: 153-154°C; ^{1}H NMR (300 MHz, DMSO-d_6) δ ppm 1.63 - 1.74 (m, 2 H, C7$\underline{H}_2$), 1.76 - 1.86 (m, 2 H, C8$\underline{H}_2$), 3.15 (s, 3 H, N3C$\underline{H}_3$), 3.24 - 3.28 (m, 2 H, C9$\underline{H}_2$), 3.31 (s, 3 H, N1C$\underline{H}_3$), 4.23 - 4.29 (m, 2 H, C6$\underline{H}_2$), 4.73 (s, 2 H, N10C$\underline{H}_2$), 7.29 - 7.36 (m, 2 H,C4H, C5H, phe), 7.41 - 7.47 (m, 1 H, C6H, phe), 7.49 - 7.52 (m, 1 H, C3H, phe); ^{13}C NMR (DMSO-d_6) δ ppm: 26.2 (C7), 27.8 (N3CH_3), 28.7 (C8), 29.8 (N1CH_3), 45.7 (C6), 51.5 (C9), 53.8 (N10CH_2), 103.9 (C4a), 127.7 (C3, phe), 129.5 (C6, phe), 129.9 (C4, phe), 130.5 (C5, phe), 133.3 (C2, phe), 135.6 (C1, phe), 147.8 (C11a), 151.4 (C2), 157.8 (C4), 158.7 (C10a); UPLC/MS purity 96.89 %; t_R = 6.38; $C_{18}H_{20}ClN_5O_2$; MW 373.83; $[M+H]^+$ 374.21

10-(2-fluorobenzyl)-1,3-dimethyl-7,8,9,10-tetrahydro-1*H*-[1,3]diazepino[2,1-*f*]purine-2,4(3*H*,6*H*)-dione (10b)

Yield: 132 mg; 68 %; mp: 120-121°C; ^{1}H NMR (400 MHz, DMSO-d_6) δ ppm 1.69 - 1.74 (m, 2 H, C7$\underline{H}_2$), 1.79 - 1.86 (m, 2 H, C8$\underline{H}_2$), 3.17 (s, 3 H, N3C$\underline{H}_3$), 3.26 - 3.31 (m, 2 H, C9$\underline{H}_2$), 3.34 (s, 3 H, N1C$\underline{H}_3$), 4.24 - 4.29 (m, 2 H, C6$\underline{H}$), 4.72 (s, 2 H, N10C$\underline{H}_2$), 7.16 - 7.25 (m, 2 H, C4H, C5H, phe), 7.31 - 7.38 (m, 1 H, C6H, phe), 7.47 - 7.54 (m, 1 H, C3H, phe); ^{13}C NMR (DMSO-d_6) δ ppm: 26.2 (C7), 27.8 (N3CH_3), 28.7 (C8), 29.8 (N1CH_3), 45.7 (C6), 49.8 (C9), 51.3 (N10CH_2), 103.8 (C4a),115.8 (d, $^{2}J_{C,F}$ = 21.3 Hz, C3, phe), 124.9 (d, $^{2}J_{C,F}$ = 3 Hz, C5, phe), 125.2 (d, $^{2}J_{C,F}$ = 13,9 Hz, C1, phe), 129.8 (d, $^{3}J_{C,F}$ = 8.1 Hz, C4, phe), 130.8 (d, $^{3}J_{C,F}$ = 4.5 Hz, C6, phe), 147.8 (C11a), 151.4 (C2), 153.9 (C4), 158.8 (C10a)), 161.1 (d, $^{1}J_{C,F}$ =245.1 Hz, C2, phe); UPLC/MS purity 100.00%; t_R = 6.35, $C_{18}H_{20}FN_5O_2$, MW 357.38, $[M+H]^+$ 358.1.

10-(3-bromobenzyl)-1,3-dimethyl-7,8,9,10-tetrahydro-1*H*-[1,3]diazepino[2,1-*f*]purine-2,4(3*H*,6*H*)-dione (10c)

Yield: 141 mg; 62 %; mp: 125-126°C; ^{1}H NMR (400 MHz, CHLOROFORM-*d*) δ ppm 1.78 - 1.85 (m, 2 H, C7$\underline{H}_2$), 1.88 - 1.94 (m, 2 H, C8$\underline{H}_2$), 3.14 - 3.18 (m, 2 H, C9$\underline{H}_2$), 3.40 (s, 3 H, N3C$\underline{H}_3$), 3.54 (s, 3 H, N1C$\underline{H}_3$), 4.39 - 4.44 (m, 2 H, C6$\underline{H}_2$), 4.67 (s, 2 H, N10C$\underline{H}_2$), 7.20 - 7.26 (m, 1 H, C6H, phe), 7.33 (d, *J*=7.82 Hz, 1 H, C5H, phe), 7.44 (d, *J*=7.82 Hz, 1 H, C4H, phe), 7.57 (s, 1 H, C2H, phe); ^{13}C NMR (CHLOROFORM-*d*) δ ppm: 26.5 (C7), 27.7 (N3CH_3), 29.2 (C8), 29.7 (N1CH_3), 45.9 (C6), 51.1 (C9), 55.9 (N10CH_2), 104.5 (C4a), 122.7 (C3, phe), 126.9 (C6, phe), 130.1 (C4, phe), 130.7 (C5, phe), 131.4 (C2, phe), 140.1 (C1, phe), 147.7 (C11a), 151.8 (C2), 154.6 (C4), 158.9 (C10a); UPLC/MS purity 100.0 %; t_R = 7.13; $C_{18}H_{20}BrN_5O_2$; MW 418.29; $[M+H]^+$ 418.3

10-(3,4-dichlorobenzyl)-1,3-dimethyl-7,8,9,10-tetrahydro-1*H*-[1,3]diazepino[2,1-*f*]purine-2,4(3*H*,6*H*)-dione (10d)

Yield: 143 mg; 64 %; mp: 147-149°C; ^{1}H NMR (300 MHz, DMSO-d_6) δ ppm 1.74 (br. s., 2 H, C7$\underline{H}_2$), 1.77 - 1.83 (m, 2 H, C8$\underline{H}_2$), 3.16 (s, 3 H, N3C$\underline{H}_3$), 3.17 - 3.21 (m, 2 H, C9$\underline{H}_2$), 3.33 (s, 3 H, N1C$\underline{H}_3$), 4.25 - 4.29 (m, 2 H, C6$\underline{H}_2$), 4.63 (s, 2 H, N10C$\underline{H}_2$), 7.43 (dd, *J*=8.21, 2.34 Hz, 1 H, C6H, phe), 7.59 (d, *J*=8.79 Hz, 1 H, C2H, phe), 7.70 (d, *J*=1.76 Hz, 1 H, C2H, phe); ^{13}C NMR (CHLOROFORM-*d*) δ ppm: 26.2 (C7), 27.8 (N3CH_3), 28.7 (C8), 29.8 (N1CH_3), 45.8 (C6), 51.1 (C9), 54.8 (N10CH_2), 103.9 (C4a), 129.0 (C3, phe), 130.3 (C6, phe), 130.7 (C4, phe), 131.0 (C5, phe), 131.4 (C2, phe), 139.8 (C1, phe), 147.7 (C11a), 151.4 (C2), 153.9 (C4), 158.8 (C10a); UPLC/MS purity 97.69 %; t_R = 7.62; $C_{18}H_{19}Cl_2N_5O_2$; MW 408.28; $[M]^+$ 408.12

10-(2-bromobenzyl)-1,3-dimethyl-7,8,9,10-tetrahydro-1*H*-[1,3]diazepino[2,1-*f*]purine-2,4(3*H*,6*H*)-dione (10e)

Yield: 146 mg; 64 %; mp: 154-155°C; ^{1}H NMR (400 MHz, CHLOROFORM-*d*) δ ppm 1.75 - 1.81 (m, 2 H, C7$\underline{H}_2$), 1.88 - 1.93 (m, 2 H, C8$\underline{H}_2$), 3.22 - 3.26 (m, 2 H, C9$\underline{H}_2$), 3.39 (s, 3 H, N3C$\underline{H}_3$), 3.54 (s, 3 H, N1C$\underline{H}_3$), 4.36 - 4.43 (m, 2 H, C6$\underline{H}_2$), 4.79 (s, 2 H, N10C$\underline{H}_2$), 7.15 - 7.21 (m, 1 H, C6H, phe), 7.31 (td, *J*=7.53, 1.37 Hz, 1 H, C4H, phe), 7.45 (dd, *J*=7.43, 1.56 Hz, 1 H, C5H, phe), 7.60 (dd, *J*=7.82, 1.17 Hz, 1 H, C3H, phe); ^{13}C NMR (CHLOROFORM-*d*) δ ppm: 26.5 (C7), 27.7 (N3CH_3), 29.0 (C8), 29.7 (N1CH_3), 45.9 (C6), 51.5 (C9), 56.4 (N10CH_2), 104.5 (C4a), 124.3 (C2, phe), 127.4 (C5, phe), 129.2 (C4, phe), 130.5 (C6, phe), 133.2 (C3, phe), 136.7 (C1, phe), 147.8 (C11a), 151.8 (C2), 154.6 (C4), 158.8 (C10a); UPLC/MS purity 99.5 %; t_R = 6.99; $C_{18}H_{20}BrN_5O_2$; MW 418.29; $[M+H]^+$ 420.09

10-(3-bromo-4-fluorobenzyl)-1,3-dimethyl-7,8,9,10-tetrahydro-1*H*-[1,3]diazepino[2,1-*f*]purine-2,4(3*H*,6*H*)-dione (10f)

Yield: 179 mg; 75 %; mp: 152-153°C; ^{1}H NMR (400 MHz, CHLOROFORM-*d*) δ ppm 1.79 - 1.85 (m, 2 H, C7$\underline{H}_2$), 1.89 - 1.94 (m, 2 H, C8$\underline{H}_2$), 3.13 - 3.17 (m, 2 H, C9$\underline{H}_2$), 3.40 (s, 3 H, N3C$\underline{H}_3$), 3.54 (s, 3 H, N1C$\underline{H}_3$), 4.39 - 4.43 (m, 2 H, C6$\underline{H}_2$), 4.64 (s, 2 H, N10C$\underline{H}_2$), 7.11 (t, *J*=8.41 Hz, 1 H, C6H, phe), 7.34 (ddd, *J*=8.31, 4.79, 2.15 Hz, 1 H, C2H, phe), 7.64 (dd, *J*=6.65, 2.35 Hz, 1 H, C5H, phe); ^{13}C NMR (CHLOROFORM-*d*) δ ppm: 26.4 (C7), 27.73 (N3CH_3), 29.2 (C8), 29.7 (N1CH_3), 45.9 (C6), 51.1 (C9), 55.3 (N10CH_2), 104.5 (C4a), 109.1 (d, $^{2}J_{C,F}$ = 21.3 Hz, C3, phe), 116.5 (d, $^{2}J_{C,F}$ = 22.8 Hz, C5, phe), 128.9 (d, $^{3}J_{C,F}$ = 7.3 Hz, C6, phe), 133.5 (C1, phe), 135.2 (d, $^{4}J_{C,F}$ = 3.6 Hz, C1, phe), 147.7 (C11a), 151.76 (C2), 154.6 (C4), 158.7 (C10a), 159.7 (C4, phe); UPLC/MS purity 95.2 %; t_R = 7.16; $C_{18}H_{19}BrFN_5O_2$; MW 436.27; $[M]^+$ 436.38

10-(2-methoxybenzyl)-1,3-dimethyl-7,8,9,10-tetrahydro-1*H*-[1,3]diazepino[2,1-*f*]purine-2,4(3*H*,6*H*)-dione (10g)

Yield: 128 mg; 63 %; mp: 157-159°C; ^{1}H NMR (400 MHz, CHLOROFORM-*d*) δ ppm 1.73 - 1.78 (m, 2 H, C7$\underline{H}_2$), 1.87 - 1.92 (m, 2 H, C8$\underline{H}_2$), 3.24 - 3.27 (m, 2 H, C9$\underline{H}_2$), 3.40 (s, 3 H, N3C$\underline{H}_3$), 3.55 (s, 3 H, N3C$\underline{H}_3$), 3.85 (s, 3 H, OC$\underline{H}_3$), 4.34 - 4.38 (m, 2 H, C6$\underline{H}_2$), 4.75 (s, 2 H, N10C$\underline{H}_2$), 6.90 - 6.96 (m, 2 H, CC4H, C5H, phe), 7.24 - 7.33 (m, 1 H, C6H, phe), 7.38 (dd, *J*=7.43, 1.56 Hz, 1 H, C3H, phe); ^{13}C NMR (CHLOROFORM-*d*) δ ppm: 26.5 (C7), 27.7 (N3CH_3), 28.9 (C8), 29.7 (N1CH_3), 45.9 (C6), 50.9 (C9), 51.2 (N10CH_2), 55.3 (O$\underline{C}H_3$), 104.3 (C4a), 110.4 (C3, phe), 120.4 (C5, phe), 125.9 (C1, phe), 128.6 (C4, phe), 129.5 (C6, phe), 148.2 (C11a), 151.9 (C2), 154.4 (C4), 157.7 (C2, phe), 159.5 (C10a); UPLC/MS purity 97.5 %; t_R = 6.36; $C_{19}H_{23}N_5O_3$; MW 369.41; $[M+H]^+$ 370.17

10-(2,4-dichlorobenzyl)-1,3-dimethyl-7,8,9,10-tetrahydro-1*H*-[1,3]diazepino[2,1-*f*]purine-2,4(3*H*,6*H*)-dione (10h)

Yield: 131 mg; 59 %; mp: 204-205°C; ^{1}H NMR (400 MHz, CHLOROFORM-*d*) δ ppm 1.78 - 1.83 (m, 2 H, C7$\underline{H}_2$), 1.88 - 1.93 (m, 2 H, C8$\underline{H}_2$), 3.20 - 3.25 (m, 2 H, C9$\underline{H}_2$), 3.39 (s, 3 H, N3C$\underline{H}_3$), 3.53 (s, 3 H, N1C$\underline{H}_3$), 4.37 - 4.41 (m, 2 H, C6$\underline{H}_2$), 4.77 (s, 2 H, N10C$\underline{H}_2$), 7.24 (dd, *J*=8.22, 1.96 Hz, 1 H, C3H, phe), 7.40 - 7.44 (m, 2 H, C5H, C6H, phe); ^{13}C NMR (CHLOROFORM-*d*) δ ppm: 26.4 (C7), 27.7 (N3CH_3), 29.1 (C8), 29.6 (N1CH_3), 45.9 (C6), 51.9 (C9), 53.6 (N10CH_2), 104.5 (C4a), 127.1 (C5, phe), 129.6 (C3, phe), 131.2 (C6, phe), 133.9 (C4, phe), 134.0 (C2, phe), 134.8 (C1, phe), 147.7 (C11a), 151.8 (C2), 154.6 (C4), 158.6 (C10a); UPLC/MS purity 97.62 %; t_R = 7.75; $C_{18}H_{19}Cl_2N_5O_2$; MW 408.28; $[M]^+$ 408.3

10-(4-chlorobenzyl)-1,3-dimethyl-7,8,9,10-tetrahydro-1*H*-[1,3]diazepino[2,1-*f*]purine-2,4(3*H*,6*H*)-dione (10i)

Yield: 121 mg; 59 %; mp: 182-183°C; ^{1}H NMR (300 MHz, DMSO-d_6) δ ppm 1.67 - 1.75 (m, 2 H, C7$\underline{H}_2$), 1.77 - 1.83 (m, 2 H, C8$\underline{H}_2$), 3.16 (s, 3 H, N3C$\underline{H}_3$), 3.17 - 3.21 (m, 2 H, C9$\underline{H}_2$), 3.33 (s, 3 H, N1C$\underline{H}_3$), 4.24 - 4.29 (m, 2 H, C6$\underline{H}_2$), 4.63 (s, 2 H, N10C$\underline{H}_2$), 7.35 - 7.41 (m, 2 H, C2H, C6H, phe), 7.42 - 7.47 (m, 2 H, C3H, C5H, phe); ^{13}C NMR (CHLOROFORM-*d*) δ ppm: 26.2 (C7), 27.8 (N3CH_3), 28.6 (C8), 29.8 (N1CH_3), 45.7 (C6), 50.9 (C9), 55.1 (N10CH_2), 103.2 (C4a), 125.58 (C2, phe), 128.8 (C5, phe), 130.4 (C4, phe), 132.3 (C6, phe), 137.5 (C3, phe), 140.3 (C1, phe), 145.1 (C11a), 147.8 (C2), 153.9 (C4), 158.9 (C10a); UPLC/MS purity 98.7 %; t_R = 7.02; $C_{18}H_{20}ClN_5O_2$; MW 373.83; $[M+H]^+$ 374.36

4.2. Biological experiments

4.2.1. Radioligand binding assays at adenosine receptors

AR radioligand binding assays were performed as previously described [38] using rat brain cortical membrane preparations for rat A_1 AR assays. Frozen rat brains (unstripped) were obtained from Pel-Freez, Rogers, Arkansas, USA. For assays at all four human AR subtypes, cell membranes of HEK or CHO cells recombinantly expressing the respective receptors were purchased from PerkinElmer.The following compounds were employed as radioligands: A_1: [^{3}H]2-Chloro-N^6-cyclopentyladenosine ([^{3}H]CCPA) [36]; A_{2A}: [^{3}H]3-(3-hydroxypropyl)-1-propargyl-7-methyl-8-(*m*-methoxystyryl)xanthine ([^{3}H]MSX-2) [37]; A_{2B}: [^{3}H]8-(4-(4-(4-chlorophenyl)-piperazine-1-sulfonyl)phenyl)-1-propylxanthine ([^{3}H]PSB-603) [38]; A_3: [^{3}H]2-phenyl-8-ethyl-4-methyl-(8*R*)-4,5,7,8-tetrahydro-1*H*-imidazo[2,1-*i*]purine-5-one ([^{3}H]PSB-11) [39]. Initially, a single high concentration of compound was tested. For potent compounds, full concentration-inhibition curves were determined using different concentrations of test compounds spanning 3 orders of magnitude. At least three independent experiments were performed. Data were analyzed using the PRISM program version 4.0 or higher (Graph Pad, San Diego, CA, USA).

4.2.2. Monoamine Oxidase Assays

Inhibition activity of compounds was measured by a fluorometric method for detecting monoamine oxidase activity using the Amplex™ Red Monoamine Oxidase Assay (ThermoFisher Scientific A12214) in a 96-well plate. Human recombinant MAO-B and MAO-A enzymes (Sigma Aldrich M7441 and M7316) were used. The assays were conducted as previously described [26].

4.2.3. Hepatotoxicity

Hepatoma HepG2 (ATCC HB-8065) cell line was kindly donated by the Department of Pharmacological Screening, Jagiellonian University Medical College. To determine the antiproliferative effect the HepG2 cells were seeded first in 96-well cell culture plate at concentration of 1.5×10^4 cells/well in glucose (4.5 g/L) and FBS (10%) supplemented Minimum Essential Medium Eagle (MEM) media (Gibco, Carlsbad, CA, USA) and incubated at 37°C for 24 hours at 5% CO_2. Next, the reference toxins and tested compounds were diluted in the same media and added to the cells. After 72h of incubation CellTiter 96® AQueous Non-Radioactive Cell Proliferation Assay (Promega, Madison, WI, USA) was added to the each well, and the cells were incubated under the same conditions for 2 h. The absorbance of the samples was measured using a microplate reader EnSpire (PerkinElmer, Waltham, MA USA) at 490 nm. The statistical significance was analyzed by GraphPad Prism™ software (version 5.01, San Diego, CA, USA) using One-way ANOVA and Bonferroni's Multiple Comparison Post Test.

4.2.4. Determination of the antioxidant activity by FRAP assay

The FRAP assay was done according to Benzie and Strain [54] with some modifications. The stock solutions included 300mM acetate buffer (3.1 g $C_2H_3NaO_2 \cdot 3H_2O$ and 16 ml $C_2H_4O_2$), pH 3.6, 10 mM TPTZ (2,4,6-tripyridyl-s-triazine) solution in 40 mM HCl, and 20 mM $FeCl_3 \cdot 6H_2O$ solution was prepared by mixing 10 parts of acetate buffer, 1 part of TPTZ solution, and 1 part of $FeCl_3 \cdot 6H_2O$ solution. 300 ul of the FRAP solution was mixed with 10 ul of tested compound solution and incubated in room temperature for 10 min in the dark condition. Readings of the colored product [ferrous tripyridyltriazine complex] were then taken at 593 nm according to ethanol. Results for tested compounds are expressed as an increase in absorbance of the test sample compared to a sample containing the solvent. Trolox was used as reference compound, which the ability to inhibit lipid peroxidation was determined in the concentration range of 1 to 300 mM.

In the FRAP assay, the antioxidant potential of sample was determined from a standard curve plotted using $FeSO_4 \cdot 7H_2O$ at a concentration range between 37.5 and 1200 µM.

4.2.5. Antioxidant effect - measurement of lipid peroxidation in rat brain homogenate

The rat brain homogenate was made in 0.9% saline containing 10 mg tissue/ml. The rates of membrane lipid peroxidation were measured by the formation of TBARS. Rat brain homogenates (1 ml) were incubated at 37°C for 5 min with 10 µl of a test compound or vehicle. Lipid peroxidation was initiated by the addition of 50 µl of 0.5 mM $FeCl_2$ and 50 µl of 2 mM ascorbic acid. After 30 min of incubation, the reaction was stopped by adding 0.1 ml of 0.2% BHT. Thiobarbituric acid reagent was then added and the mixture was heated for 15 min in a boiling water bath. The TBARS was extracted by n-butanol and measured at 532 nm. The amount of TBARS was quantified using a standard curve of MDA as described previously.[55]

4.3. Molecular docking

For docking purposes, Schrödinger Maestro Suite was used [46]. Ligands were built in their 3D forms and their bioactive conformations were generated using ConfGen module [47,48](water environment, target number of conformers – 20). Crystal structures: 3REY and 2V5Z were prepared for docking using Protein Preparation Wizard [49], ligand binding sites were centered on bound ligands. Docking to rigid form of receptor was performed using Glide module [50–52] (precision standard, flexible ligand sampling, max 5 poses per conformer). Ligands were rated according their position in binding pocket, interactions with

binding pocket amino acids as well as the docking score value. Ligand interaction diagrams were generated using Schrödinger Maestro, ligand-receptor visualizations were generated using UCSF Chimera [53].

Acknowledgements

Financial support by the Jagiellonian University Medical College [grant no. K/DSC/003511, K/ZDS/007121], Polish National Science Center grant based on decision No DEC-2016/23/N/NZ7/00475 are gratefully acknowledged. We thank Anika Püsche, Angelika Fischer, Alexandra Jünger-Leif, and Christin Vielmuth for expert technical assistance in compound testing. Thanks are due to the European Commission for funding our collaboration within the COST Action MuTaLig.

Supplementary data

Supplementary data associated with this article can be found, in the online version, at ....

References and notes

1. Ballard C, Gauthier S, Corbett A, Brayne C, Aarsland D, Jones E. Alzheimer's disease. Lancet. 2011;377(9770):1019–31. http://dx.doi.org/10.1016/S0140-6736(10)61349-9

2. Kakkar AK, Dahiya N. Management of Parkinson′s disease: Current and future pharmacotherapy. Eur J Pharmacol. 2015 Mar;750:74–81. http://dx.doi.org/10.1016/j.ejphar.2015.01.030

3. Jenkins TM, Hollinger H, McDermott CJ. The evidence for symptomatic treatments in amyotrophic lateral sclerosis. Curr Opin Neurol. 2014;27(5):524–31.

4. Gövert F, Schneider SA. Huntington,s disease and Huntington,s disease-like syndromes: An overview. Curr Opin Neurol. 2013;26(4):420–7.

5. Schapira AH. Mitochondrial dysfunction in neurodegenerative diseases. Neurochem Res. 2008;33(12):2502–9. http://www.ncbi.nlm.nih.gov/pubmed/18998208

6. Bar-am O, Amit T, Kupershmidt L, Aluf Y, Mechlovich D, Kabha H, et al. Neurobiology of Aging Neuroprotective and neurorestorative activities of a novel iron chelator-brain selective monoamine oxidase-A / monoamine oxidase-B inhibitor in animal models of Parkinson ' s disease and aging. Neurobiol Aging. 2015;36(3):1529–42. http://dx.doi.org/10.1016/j.neurobiolaging.2014.10.026

7. Mulligan VK, Chakrabartty A. Protein misfolding in the late-onset neurodegenerative diseases: Common themes and the unique case of amyotrophic lateral sclerosis. Proteins Struct Funct Bioinforma. 2013;81(8):1285–303.

8. Pisani L, Catto M, Leonetti F, Nicolotti O, Stefanachi A, Campagna F, et al. Targeting monoamine oxidases with multipotent ligands: an emerging strategy in the search of new drugs against neurodegenerative diseases. Curr Med Chem. 2011;18(30):4568–87. http://www.ncbi.nlm.nih.gov/pubmed/21864289

9. Freitas ME, Fox SH. Nondopaminergic treatments for Parkinson's disease: current and future prospects. Neurodegener Dis Manag. 2016 Jun;6(3):249–68. http://www.futuremedicine.com/doi/10.2217/nmt-2016-0005

10. Cavalli A, Bolognesi ML, Mìnarini A, Rosini M, Tumiatti V, Recanatini M, et al. Multi-target-directed ligands to combat neurodegenerative diseases. J Med Chem. 2008;51(3):347–72.

11. Petzer JP, Castagnoli N, Schwarzschild M a, Chen J. Dual-Target – Directed Drugs that Block Monoamine Oxidase B and Adenosine A2A Receptors for Parkinson's Disease. Neurotherapeutics. 2009;6:141–51.

12. Song B, Xiao T, Qi X, Li L, Qin K, Nian S, et al. Bioorganic & Medicinal Chemistry Letters Design and synthesis of 8-substituted benzamido-phenylxanthine derivatives as MAO-B inhibitors. Bioorg Med Chem Lett. 2012;22(4):1739–42. http://dx.doi.org/10.1016/j.bmcl.2011.12.094

13. Toprakçí M, Yelekçi K. Docking studies on monoamine oxidase-B inhibitors: Estimation of inhibition constants (Ki) of a series of experimentally tested compounds. Bioorg Med Chem Lett. 2005 Oct;15(20):4438–46. http://linkinghub.elsevier.com/retrieve/pii/S0960894X05009261

14. Mertens MD, Hinz S, Müller CE, Gütschow M. Alkynyl-coumarinyl ethers as MAO-B inhibitors. Bioorganic Med Chem. 2014;22(6):1916–28.

15. Strydom B, Bergh JJ, Petzer JP. European Journal of Medicinal Chemistry 8-Aryl- and alkyloxycaffeine analogues as inhibitors of monoamine oxidase. Eur J Med Chem. 2011;46(8):3474–85. http://dx.doi.org/10.1016/j.ejmech.2011.05.014

16. Finberg JPM. Update on the pharmacology of selective inhibitors of MAO-A and MAO-B: Focus on modulation of CNS monoamine neurotransmitter release. Pharmacol Ther. 2014;143(2):133–52. http://dx.doi.org/10.1016/j.pharmthera.2014.02.010

17. Talati R, Reinhart K, Baker W, White CM, Coleman CI. Pharmacologic treatment of advanced Parkinson's disease: A meta-analysis of COMT inhibitors and MAO-B inhibitors. Park Relat Disord. 2009;15(7):500–5. http://dx.doi.org/10.1016/j.parkreldis.2008.12.007

18. Carradori S, Petzer JP. Novel monoamine oxidase inhibitors: a patent review (2012 – 2014). Expert Opin Ther Pat. 2014;1–20. http://www.tandfonline.com/doi/full/10.1517/13543776.2014.982535

19. Fredholm BB, IJzerman AP, Jacobson KA, Linden J, Muller CE. International Union of Basic and Clinical Pharmacology. LXXXI. Nomenclature and Classification of Adenosine Receptors--An Update. Pharmacol Rev. 2011 Mar 1;63(1):1–34. http://pharmrev.aspetjournals.org/cgi/doi/10.1124/pr.110.003285

20. Jacobson KA, Gao ZG. Adenosine receptors as therapeutic targets. Nat Rev Drug Discov. 2006;5(3):247–64.

21. Fuxe K, Marcellino D, Borroto-Escuela DO, Guescini M, Fernández-Dueñas V, Tanganelli S, et al. Adenosine-Dopamine Interactions in the Pathophysiology and Treatment of CNS Disorders. CNS Neurosci Ther. 2010 May 6;16(3):e18–42. http://doi.wiley.com/10.1111/j.1755-5949.2009.00126.x

22. Yu L, Shen HY, Coelho JE, Araújo IM, Huang QY, Day YJ, et al. Adenosine A2A receptor antagonists exert motor and neuroprotective effects by distinct cellular mechanisms. Ann Neurol. 2008;63(3):338–46.

23. Rivera-Oliver M, Díaz-Ríos M. Using caffeine and other adenosine receptor antagonists and agonists as therapeutic tools against neurodegenerative diseases: A review. Life Sci. 2014;101(1–2):1–9. http://dx.doi.org/10.1016/j.lfs.2014.01.083

24. Bonaventura J, Rico AJ, Moreno E, Sierra S, Sánchez M, Luquin N, et al. L-DOPA-treatment in primates disrupts the expression of A2A adenosine-CB1 cannabinoid-D2 dopamine receptor heteromers in the caudate nucleus. Neuropharmacology. 2014;79:90–100. http://dx.doi.org/10.1016/j.neuropharm.2013.10.036

25. Laurent C, Eddarkaoui S, Derisbourg M, Leboucher A, Demeyer D, Carrier S, et al. Beneficial effects of caffeine in a transgenic model of Alzheimer's disease-like tau pathology. Neurobiol Aging. 2014;35(9):2079–90. http://dx.doi.org/10.1016/j.neurobiolaging.2014.03.027

26. Stößel A, Schlenk M, Hinz S, Küppers P, Heer J, Gütschow M, et al. Dual targeting of adenosine A2A receptors and monoamine oxidase B by 4H-3,1-benzothiazin-4-ones. J Med Chem. 2013;56(11):4580–96.

27. Van Der Walt MM, Terre'Blanche G, Petzer A, Petzer JP. The adenosine receptor affinities and monoamine oxidase B inhibitory properties of sulfanylphthalimide analogues. Bioorg Chem. 2015;59:117–23. http://dx.doi.org/10.1016/j.bioorg.2015.02.005

28. Rivara S, Piersanti G, Bartoccini F, Diamantini G, Pala D, Riccioni T, et al. Synthesis of (E)-8-(3-chlorostyryl)caffeine analogues leading to 9-deazaxanthine derivatives as dual A2A antagonists/MAO-B inhibitors. J Med Chem. 2013;56(3):1247–61.

29. Dungo R, Deeks ED. Istradefylline: First Global Approval. Drugs. 2013 Jun 23;73(8):875–82. http://link.springer.com/10.1007/s40265-013-0066-7

30. Szymańska E, Drabczyńska A, Karcz T, Müller CE, Köse M, Karolak-Wojciechowska J, et al. Similarities and differences in affinity and binding modes of tricyclic pyrimido- and pyrazinoxanthines at human and rat adenosine receptors. Bioorg Med Chem . 2016 Sep;24(18):4347–62. http://linkinghub.elsevier.com/retrieve/pii/S0968089616305351

31. Drabczyńska A, Schumacher B, Müller CE, Karolak-Wojciechowska J, Michalak B, Pękala E, et al. Impact of the aryl substituent kind and distance from pyrimido[2,1-f]purindiones on the adenosine receptor selectivity and antagonistic properties. Eur J Med Chem. 2003 Apr;38(4):397–402. http://linkinghub.elsevier.com/retrieve/pii/S0223523403000515

32. Eva-Marìa Priego, Jacobien von Frijtag Drabbe Kuenzel, Ad P. IJzerman, Marìia-Jose´ Camarasa A, Pèrez-Pèrez M-J. Pyrido[2,1-f]purine-2,4-dione Derivatives as a Novel Class of Highly Potent Human A3 Adenosine Receptor Antagonists. J Med Chem. 2002;(45):3337–44.

33. Koch P, Akkari R, Brunschweiger A, Borrmann T, Schlenk M, Küppers P, et al. 1,3-Dialkyl-substituted tetrahydropyrimido[1,2-f]purine-2,4-diones as multiple target drugs for the potential treatment of neurodegenerative diseases. Bioorg Med Chem. 2013 Dec;21(23):7435–52. http://linkinghub.elsevier.com/retrieve/pii/S0968089613008249

34. Drabczyńska A, Müller CE, Lacher SK, Schumacher B, Karolak-Wojciechowska J, Nasal A, et al. Synthesis and biological activity of tricyclic aryloimidazo-, pyrimido-, and diazepinopurinediones. Bioorganic Med Chem. 2006;14(21):7258–81.

35. Drabczyńska A, Yuzlenko O, Köse M, Paskaleva M, Schiedel AC, Karolak-Wojciechowska J, et al. Synthesis and biological activity of tricyclic cycloalkylimidazo-, pyrimido- and diazepinopurinediones. Eur J Med Chem. 2011 Sep;46(9):3590–607. http://linkinghub.elsevier.com/retrieve/pii/S0223523411004016

36. Martin KK, Ulrich JL, Cristalli G, Vittori S, Grifantini M. Archives of Pharmacology a high affinity agonist radioligand for A1 adenosine receptors. 1989;679–83.

37. Müller CE, Maurinsh J, Sauer R. Binding of [3H]MSX-2 (3-(3-hydroxypropyl)-7-methyl-8-(m-methoxystyryl)-1-propargylxanthine) to rat striatal membranes--a new, selective antagonist radioligand for A(2A) adenosine receptors. Eur J Pharm Sci. 2000;10(4):259–65. http://www.ncbi.nlm.nih.gov/pubmed/10838015

38. Borrmann T, Hinz S, Bertarelli DCG, Li W, Florin NC, Scheiff AB, et al. 1-Alkyl-8-(piperazine-1-sulfonyl)phenylxanthines: Development and characterization of adenosine A2B receptor antagonists and a new radioligand with subnanomolar affinity and subtype specificity. J Med Chem. 2009 Jul 9;52(13):3994–4006. http://pubs.acs.org/doi/abs/10.1021/jm900413e

39. Müller CE, Diekmann M, Thorand M, Ozola V. [3H]8-Ethyl-4-methyl-2-phenyl-(8R)-4,5,7,8-tetrahydro-1H-imidazo [2,1-i]-purin-5-one ([3H]PSB-11), a Novel High-Affinity Antagonist Radioligand for Human A3 Adenosine Receptors. Bioorganic Med Chem Lett. 2002;12(3):501–3.

40. Muller CE, Jacobson KA. Recent developments in adenosine receptor ligands and their potential as novel drugs. BiochimBiophysActa. 2011;1808(0006–3002):1290–308. http://dx.doi.org/10.1016/j.bbamem.2010.12.017

41. Drabczyńska A, Müller CE, Karolak-Wojciechowska J, Schumacher B, Schiedel A, Yuzlenko O, et al. N9-Benzyl-substituted 1,3-dimethyl- and 1,3-dipropyl-pyrimido[2,1-f]purinediones: Synthesis and

structure-activity relationships at adenosine A1 and A2A receptors. Bioorganic Med Chem. 2007;15(14):5003–17.

42. Cheng RKY, Segala E, Robertson N, Deflorian F, Doré AS, Errey JC, et al. Structures of Human A 1 and A 2A Adenosine Receptors with Xanthines Reveal Determinants of Selectivity. Structure [Internet]. 2017 Aug;25(8):1275–1285.e4. Available from: http://linkinghub.elsevier.com/retrieve/pii/S0969212617301922

43. Doré AS, Robertson N, Errey JC, Ng I, Hollenstein K, Tehan B, et al. Structure of the Adenosine A2A Receptor in Complex with ZM241385 and the Xanthines XAC and Caffeine. Structure. 2011 Sep;19(9):1283–93. http://linkinghub.elsevier.com/retrieve/pii/S0969212611002383

44. Drabczyńska A, Karcz T, Szymańska E, Köse M, Müller CE, Paskaleva M, et al. Synthesis, biological activity and molecular modelling studies of tricyclic alkylimidazo-, pyrimido- and diazepinopurinediones. Purinergic Signal. 2013 Sep 2;9(3):395–414. http://link.springer.com/10.1007/s11302-013-9358-3

45. Binda C, Wang J, Pisani L, Caccia C, Carotti A, Salvati P, et al. Structures of Human Monoamine Oxidase B Complexes with Selective Noncovalent Inhibitors: Safinamide and Coumarin Analogs. J Med Chem. 2007 Nov;50(23):5848–52. http://pubs.acs.org/doi/abs/10.1021/jm070677y

46. Schrödinger Release 2017-1: Schrödinger Suite 2017-1 Induced Fit Docking protocol; Glide, Schrödinger, LLC, New York, NY, 2017; Prime, Schrödinger, LLC, New York, NY, 2017.

47. Watts KS, Dalal P, Murphy RB, Sherman W, Friesner RA, Shelley JC. ConfGen: A Conformational Search Method for Efficient Generation of Bioactive Conformers. J Chem Inf Model. 2010 Apr 26;50(4):534–46. http://pubs.acs.org/doi/abs/10.1021/ci100015j

48. Schrödinger Release 2017-1: ConfGen, Schrödinger, LLC, New York, NY, 2016.

49. Schrödinger Release 2017-1: Schrödinger Suite 2017-1 Protein Preparation Wizard; Epik, Schrödinger, LLC New York, NY, 2017.

50. Schrödinger Release 2017-1: Glide, Schrödinger, LLC, New York, NY, 2017.

51. Halgren TA, Murphy RB, Friesner RA, Beard HS, Frye LL, Pollard WT, et al. Glide: A New Approach for Rapid, Accurate Docking and Scoring. 2. Enrichment Factors in Database Screening. J Med Chem. 2004 Mar;47(7):1750–9. http://pubs.acs.org/doi/abs/10.1021/jm030644s

52. Friesner RA, Murphy RB, Repasky MP, Frye LL, Greenwood JR, Halgren TA, et al. Extra Precision Glide: Docking and Scoring Incorporating a Model of Hydrophobic Enclosure for Protein−Ligand Complexes. J Med Chem. 2006 Oct;49(21):6177–96. http://pubs.acs.org/doi/abs/10.1021/jm051256o

53. Pettersen EF, Goddard TD, Huang CC, Couch GS, Greenblatt DM, Meng EC, et al. UCSF Chimera?A visualization system for exploratory research and analysis. J Comput Chem [Internet]. 2004 Oct;25(13):1605–12. Available from: http://doi.wiley.com/10.1002/jcc.20084

54. Benzie IFF, Strain JJ. The Ferric Reducing Ability of Plasma (FRAP) as a Measure of "Antioxidant Power": The FRAP Assay. Anal Biochem. 1996 Jul;239(1):70–6. http://linkinghub.elsevier.com/retrieve/pii/S0003269796902924

55. Yue TL, Cheng HY, Lysko PG, McKenna PJ, Feuerstein R, Gu JL, et al. Carvedilol, a new vasodilator and beta adrenoceptor antagonist, is an antioxidant and free radical scavenger. J Pharmacol Exp Ther. 1992 Oct;263(1):92–8. http://www.ncbi.nlm.nih.gov/pubmed/1357162CM

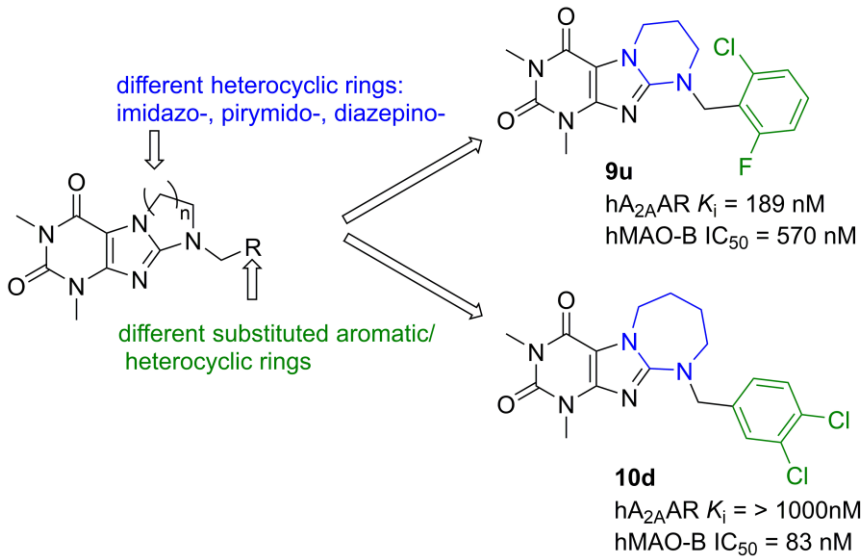

Biological experiments:

adenosine receptors
monoamine oxidase A and B
hepatotoxicty
antioxidant activity

In silio experiments:

molecular docking
physico-chemical parameters

Highlights

- Novel tricyclic xanthine derivatives were obtained as potential dual adenosine A_{2A} receptor/monoamine oxidase B ligands.
- Potent ligands of adenosine A_{2A} receptors and monoamine oxidase B with nanomolar affinities were found.
- Structure–activity relationship for the synthesized series supported by molecular docking for both targets was analyzed.
- Selected physicochemical and potential toxic properties were evaluated in *in silico* and *in vitro* studies.
- Potential antioxidant properties were estimated for selected compounds.